ISTC Reports

Illinois Sustainable Technology Center

Slurry Phase Catalysts for Bio-Oil Upgradation

Brajendra K. Sharma
Kirtika Kohli
Illinois Sustainable Technology Center

ILLINOIS
Illinois Sustainable Technology Center
PRAIRIE RESEARCH INSTITUTE

TR-077
July 2020
www.istc.illinois.edu

TR-077

Slurry Phase Catalysts for Bio-Oil Upgradation

Brajendra K. Sharma
Kirtika Kohli
Illinois Sustainable Technology Center

July 2020

Submitted to the
Illinois Sustainable Technology Center
Prairie Research Institute
University of Illinois at Urbana-Champaign
www.istc.illinois.edu

The report is available online at:
https://www.ideals.illinois.edu/handle/2142/811

Printed by the Authority of the State of Illinois
J. B. Pritzker, Governor

Acknowledgments

We are grateful for financial support from the Hazardous Waste Research Fund (Grant No. HWR18-251) that is administered by the Illinois Sustainable Technology Center, a part of the Prairie Research Institute at the University of Illinois at Urbana-Champaign. The authors acknowledge the School of Chemical Sciences at the University of Illinois for XRD and CHN analyses. TGA, SEM, Raman, and HR-TEM analyses were carried out in the Frederick Seitz Materials Research Laboratory Central Research Facilities, University of Illinois at Urbana-Champaign. The authors would like to thank Tim Leon for help in setting up the reactor and Lee Green for conducting GC-MS analysis.

Table of Contents

List of Tables

List of Figures

List of Abbreviations

AHM	Ammonium heptamolybdate
Al	Aluminum
ASTM	American Society for Testing and Materials
C	Carbon
CoMoS Cmr	Commercial cobalt molybdenum sulfide catalyst
CoMoS Slurry	Cobalt molybdenum sulfided catalysts prepared by slurry route
DCM	Dichloromethane
DTG	Derivative thermogravimetric analysis
EtOH	Ethanol
FT-IR	Fourier transform-Infrared spectroscopy
GC-MS	Gas chromatography-Mass spectrometry
H	Hydrogen
HDO	Hydrodeoxygenation
HDT	Hydrotreatment
HHV	Higher heating value
HTBCr	Hydrothermal liquefaction biocrude oil
HTL	Hydrothermal liquefaction
Mo	Molybdenum
MoS-I	Molybdenum sulfide catalyst prepared by precipitation route
MoS-II	Molybdenum sulfide catalyst prepared by hydrothermal route
MoS-OS	Oil-soluble molybdenum sulfide slurry catalyst
MoS-WS	Water-soluble molybdenum sulfide slurry catalyst
MoC	Molybdenum carbide catalyst
Ni	Nickel
NiC	Nickel carbide catalyst
NiS	Nickel sulfide catalyst
NIST	National Institute of Standards and Technology
NREL	National Renewable Energy Laboratory
O	Oxygen
P	Pressure
PBCr-I	Pyrolysis biocrude oil-I
PBCr-II	Pyrolysis biocrude oil-II
PMA	Phosphomolybdic acid
S	Sulfur
SD	Standard deviation
SEM	Scanning electron microscopy
T	Temperature
TEM	Transmission electron microscopy
TGA	Thermogravimetric analysis
THF	Tetrahydrofuran
wppm	Weight parts per million
wt%	Weight %
XRD	X-ray diffraction

Abstract

The catalytic hydrodeoxygenation (HDO) of food waste-derived biocrude oil was investigated to produce renewable hydrocarbons using slurry phase sulfide and carbide catalysts. Experiments were performed to evaluate the effectiveness of the slurry phase catalysts for the hydrotreatment of biocrude oils. The results were compared with the conventional hydrotreating sulfide catalysts supported on alumina. The dispersed catalysts showed very high hydrocracking and HDO activities for the hydrotreatment of biocrude oils. The results revealed that coke formation was reduced drastically, and the properties of the products were significantly improved with a lower oxygen content and higher heating values. The catalyst activities were compared with the commercially used bimetallic $CoMo/Al_2O_3$ catalyst at the same reaction temperature and pressure. The slurry phase catalysts were found to be effective, even at a very low concentration, i.e., wppm levels. The experimental results showed that a 2.5 wt% CoMo slurry catalyst led to a decrease in both the oxygen content and coke amount compared to 20 wt% for the conventional CoMo catalyst. Further, Mo- and Ni-based carbide dispersed catalysts were tested for the hydrotreatment (HDT) of biocrude oil, and the MoC catalyst displayed higher activity. However, the activity was less compared to the conventional $CoMo/Al_2O_3$ catalyst.

A series of different Mo-based sulfide catalysts (i.e., dispersed solid powder, oil-soluble, and water-soluble) were prepared, and the activities of the catalysts were evaluated at high-temperature / high-pressure reaction conditions for the HDT of a hydrothermal liquefaction (HTL) biocrude oil. Among these, the oil-soluble MoS_2 slurry catalyst showed the highest activity. The oil-soluble slurry catalyst was evaluated further using a different catalyst concentration, finding that this catalyst is more effective in the range of 1100 to 1700 metal wppm. Slurry catalysts are highly dispersed in the feedstock, which leads to the higher selectivity and conversions. A significant decrease in the oxygen content and an increase in liquid product demonstrated the potential use of slurry catalysts for the hydrotreatment of biocrude oils.

Chapter 1: Literature Review

Bio-oil produced by fast pyrolysis or hydrothermal liquefaction of biomass is a promising second-generation renewable energy carrier. However, due to its instability and high oxygen content, the direct use of bio-oil as a liquid fuel is currently not feasible [1-3]. Therefore, in this report this type of bio-oil is referred to as biocrude oil. The aqueous acidic (containing 15–30 wt% H_2O, pH 2.5) and highly oxygenated (nearly sulfur-free, ca. 30 wt% phenolic fraction) biocrude oil mixture [4] would be a promising basic resource if suitable catalytic technology existed for its conversion to alkanes.

Biocrude oil upgradation can be carried out using different methods, such as hydrotreating [3,5], upgrading by zeolite [6-9], aqueous-phase processing [10], or a combination of these processes [11]. Among these, hydrotreating is considered the most effective method in which biocrude oil is upgraded by hydrodeoxygenation (HDO) to produce hydrocarbons and water with the saturation of double bonds or aromatic rings by hydrogenation [12]. The typical hydrotreating reaction takes place between 400 and 773 K under high-pressure hydrogen in the presence of conventional hydrotreating sulfide-based catalysts ($CoMo/Al_2O_3$ or $NiMo/Al_2O_3$) [3,13]. However, these catalysts contaminate the products by the incorporation of sulfur and rapid deactivation by coke deposition and water present in these biocrude oils [14,15]. Conceptually, the reductive upgrading of biocrude oils in an acidic aqueous medium using novel catalysts offers a new, attractive route.

Recently, a slurry bed hydrocracking process using various dispersed catalysts has been demonstrated and proved to be superior to conventional hydrocrackers [16–22]. The catalysts used in slurry phase hydrocracking are generally sub-micronic particles of metal sulfides, and these sulfides are used either ex-situ or in-situ. In the ex-situ process, the catalysts are synthesized and then dispersed in oils. In the in-situ process, oil-soluble metal precursors are mixed with the feed. Catalyst sulfiding for the in-situ catalysts occurs by means of sulfur species that are thermally decomposed in the feedstock during the reaction [17]. The metal precursors used are typically water-soluble salts, an oil-soluble metal complex, or a fine powder solid. The sulfides of transition metals, such as molybdenum (Mo), nickel (Ni), cobalt (Co), vanadium (V), and ruthenium (Ru), are reportedly active for hydrotreating. However, molybdenum sulfide (MoS_2) is the most commonly used catalyst for hydroprocessing [23–25].

The use of slurry catalysts for biocrude oil upgradation is not reported in the literature. Therefore, the major goal of this work was to evaluate the activity of slurry phase catalysts for the upgradation of biocrude oils. In particular, the research objectives were to:

- Synthesize and characterize slurry phase catalysts using different synthesis procedures;
- Develop a process for the slurry bed hydrocracking of the biocrude oils (produced from pyrolysis and hydrothermal liquefaction processes);
- Demonstrate the feasibility of the slurry bed hydrocracking process for the upgradation of biocrude oils using synthesized catalysts;

- Determine a chemical characterization of the upgraded products using elemental analysis, thermogravimetric analyzer (TGA), Fourier Transform-Infrared (FT-IR) spectroscopy, and gas chromatography-mass spectrometer (GC-MS); and
- Study the hydrodeoxygenation (HDO) activity of the synthesized catalysts.

Chapter 2: Catalyst Synthesis and Characterizations

2.1 Catalyst Synthesis

The designations used for the synthesized catalysts to report catalyst activities in this work are presented in Table 2.1.

Table 2.1: *Designations used for the synthesized catalysts.*

CoMoS Cmr	Sulfide CoMo catalysts from previous work [15]	[15]
MoS-I	Molybdenum (Mo) sulfide catalyst prepared by precipitation route	2.1.1
MoS-II	Molybdenum (Mo) sulfide catalyst prepared by hydrothermal route	2.1.1
CoMoS Slurry	Sulfide bimetallic CoMo catalysts prepared by slurry route	2.1.2
MoS-OS	Oil-soluble Mo sulfide slurry catalyst	2.1.3
MoS-WS	Water-soluble slurry-based catalyst	2.1.3
MoC	Mo carbide catalyst	2.1.4
NiC	Ni carbide catalyst	2.1.4

2.1.1 Synthesis of Molybdenum-based Sulfide Catalysts

Molybdenum sulfide catalysts were synthesized using precipitation and hydrothermal routes. Ammonium heptamolybdate (AHM) and ammonium sulfide were used as a molybdenum precursor and a sulfiding agent, respectively. For the precipitation route, 0.0047 mol of AHM was dissolved in 50 mL of deionized water; then, 4 mL of ammonium hydroxide and 5 mL of hydrazine (reducing agent) was added to that solution. Finally, 8 mL of ammonium sulfide was added to the solution. The whole mixture was stirred at 80 °C for 2.5 h. The prepared solution was then left at room temperature overnight. The next day, the solution was evaporated at 90 °C for 1 h, and then the recovered solid material was dried in a vacuum oven at 80 °C for 12 h. The dried catalyst was then reduced in the presence of hydrogen (50 mL/min) at 400 °C for a reaction time of 2 h.

For the hydrothermal route, the procedure was similar, except after making a solution of AHM and ammonium sulfide, the solution was transferred to a 40 mL autoclave reactor. The solution was treated at 220 °C for 4 h. After the hydrothermal treatment, the solution was centrifuged, and the recovered solid was washed with ethanol three times. The solid catalyst was then dried in a vacuum oven at 80 °C for 12 h. The as-prepared catalyst was reduced in the presence of hydrogen (50 mL/min) at 400 °C for a reaction time of 2 h.

2.1.2 Synthesis of Bimetallic Cobalt Molybdenum Sulfide (CoMoS) Catalyst

The synthesis of the CoMoS slurry catalyst was performed based on the hydrothermal route (described in section 2.1.1). In this process, 0.0014 mol of AHM and 0.0019 mol of cobalt nitrate were used. The rest of the procedure was the same as for the MoS_2 hydrothermal procedure.

2.1.3 Oil-Soluble and Water-Soluble Slurry Catalysts

The oil-soluble slurry catalyst was prepared by using AHM as a molybdenum precursor and thiourea as a sulfide source. In this process, 0.0002 mol of AHM was dissolved in 40 mL of ethylene glycol, and then 0.0066 mol of thiourea was added at 45 °C with stirring. Next, 0.00084 mol of sodium oleate (surfactant) and 0.00045 mol of cetylamine were added to the solution. The as-prepared solution was stirred at 45 °C for 3 h, and then the whole mixture was transferred to a 40 mL autoclave reactor. The solution was treated at 180 °C for 6 h, and the reactor was cooled to room temperature. The solution was centrifuged to separate the black-colored solid from the solution. The black solid was washed with ethanol three times. Finally, the black solid was reduced in the presence of hydrogen (50 mL/min) at 400 °C for a reaction time of 2 h. The water-soluble slurry catalyst was synthesized using the reverse micelle method [20].

2.1.4 Synthesis of Carbide Catalysts

A molybdenum carbide catalyst was synthesized using the urea-glass route in which urea was used as a carbide source. In this synthesis procedure, molybdenum chloride (0.008 mol) was dissolved in ethanol (5 ml), and then urea (10 mol) was added to the mixture. The resulting solution was stirred at room temperature for 3 h. Next, the mixture was transferred to a petri dish and dried in a vacuum oven at 45 °C for 12 h. The dried material was then treated at 800 °C for 3 h in the presence of nitrogen.

A nickel carbide-based catalyst was prepared using nickel (II) acetylacetonate (0.0019 mol) and dissolved in a mixture of oleylamine (0.15 mol) and oleic acid (0.0290 mol). The synthesis method reported by Yang et al. [26] was used. The as-prepared solution was heated at 280 °C for 60 min. After the heat treatment, the solution was cooled to room temperature and washed using hexane. The solid was recovered via centrifugation of the whole mixture. The recovered solid was dried at 80 °C for 48 h in a vacuum oven.

2.2 Catalyst Characterizations

Thermogravimetric analysis (TGA) was conducted using a Q50 TGA from TA Instruments. The experiment was performed under nitrogen flow (60 mL/min) with 4-5 mg of sample. The sample was heated from room temperature to 900 °C at the rate of 10 °C/min. X-ray diffraction (XRD) analysis of the samples was conducted on a Rigaku Miniflex 600 diffractometer (CuKα radiation with λ=0.15418 nm). The diffraction intensities were measured in the 2θ range from 20 ° to 80 ° on a step-scan mode (0.02 °/step). Raman analysis was conducted using a Nanophoton Raman 11 analyzer at 532 nm excitation. The surface morphology of the catalysts was studied using the scanning electron microscopy (SEM) technique. SEM was performed using a JEOL 6060 LV instrument. Transmission electron microscopy (TEM) analysis was used to determine the structural properties of the catalysts and was performed with a JEOL JEM-2010 electron microscope operated at 200 Kv. The TEM samples were prepared by dispersing the synthesized

catalysts in isopropanol using ultrasonication. The small drop of dispersed catalysts was then placed on a Holey carbon-coated grid (200 mesh).

2.3 Results and Discussion

The thermal stability of the MoS_2 catalysts synthesized by precipitation (MoS-I) and hydrothermal (MoS-II) routes was studied by TGA. Weight loss against temperature is presented in Fig. 2.1. The weight loss tendencies of the synthesized catalysts were slow, as observed from the TGA curves. The thermal stabilities of the catalysts were more than 75%, and the weight losses observed in these catalysts were due to the decomposition of the precursors used for synthesis during heat treatments in TGA. It is worth mentioning here that the vacuum dried as-synthesized catalysts at 80 ˚C were used for TGA analysis. The decomposition of the catalysts can be seen from the derivative thermogravimetric (DTG) curve, as shown in Fig. 2.1. Two-step weight losses at 309 and 450 ˚C were found from the DTG curve of MoS-II, while three-step weight losses at 225, 326, and 448 ˚C were found for MoS-I. As mentioned earlier, these losses are due to the decomposition of the precursors used for the synthesis by the heat treatment used in TGA.

XRD patterns of the catalysts are shown in Fig. 2.2. The figure reveals the characteristics of wide diffraction peaks and weak intensities, which confirm their smaller size and low crystallinity [26]. A weak peak appeared around 2θ value of 33 ° for the CoMoS slurry catalyst (Fig. 2.2(i)), which can be assigned to the (100) plane of the crystalline molybdenum sulfide (2θ = 33 ° and 36 °). The XRD pattern due to the (002) plane of the crystalline MoS_2 appeared around 2θ value of 13 °, and the peak is more intense compared to the (100) plane. The XRD pattern reveals the poor crystallinity of the bimetallic CoMoS slurry catalyst.

In the case of the catalyst synthesized by the precipitation route (MoS-I), the intensity of the diffraction peaks becomes sharper, indicating the improvement in crystallinity. On comparing the XRD patterns with the reported literature, it was observed that all peaks in the MoS-II catalyst were significantly broader than in the pristine 2H-MoS_2 (JCPDS card No. 73-1508) [27]. The broader peaks were most likely due to the poor crystallinity and smaller particle size. The intensity of the (100) plane was more intense in the MoS-I as compared to the MoS-II catalyst (Fig. 2.2(ii)).

For the NiC catalyst (Fig. 2.2(iii)), an intense peak of Ni (200) metal at 43 ° was observed. The XRD peaks observed in NiC indicate a similarity with Ni_3C (No. 06-0697), metallic Ni with hexagonal (No. 45-1027), and fcc (No. 04-0850) structures [28].

The Raman spectra of the MoS-II catalyst were recorded and are provided in Fig. 2.3. The indicators of in-plane (E^1_{2g}) and out-of-plane (A_{1g}) vibration modes of the sulfur atoms were located in the region 300-400 cm^{-1} and are for single-layer MoS_2. The spectra were consistent with the literature.

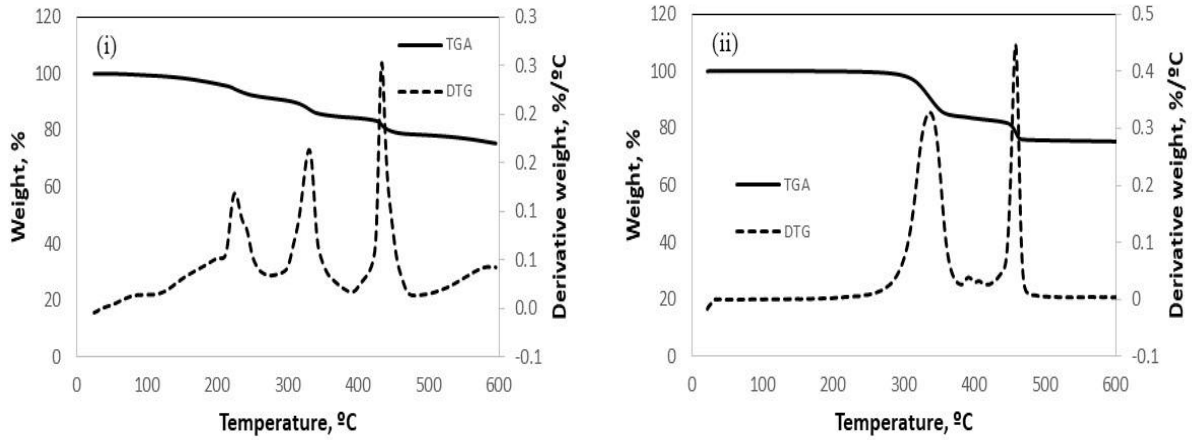

Figure 2.1: *TGA-DTG curves for the synthesized catalysts (i) MoS-I and (ii) MoS-II.*

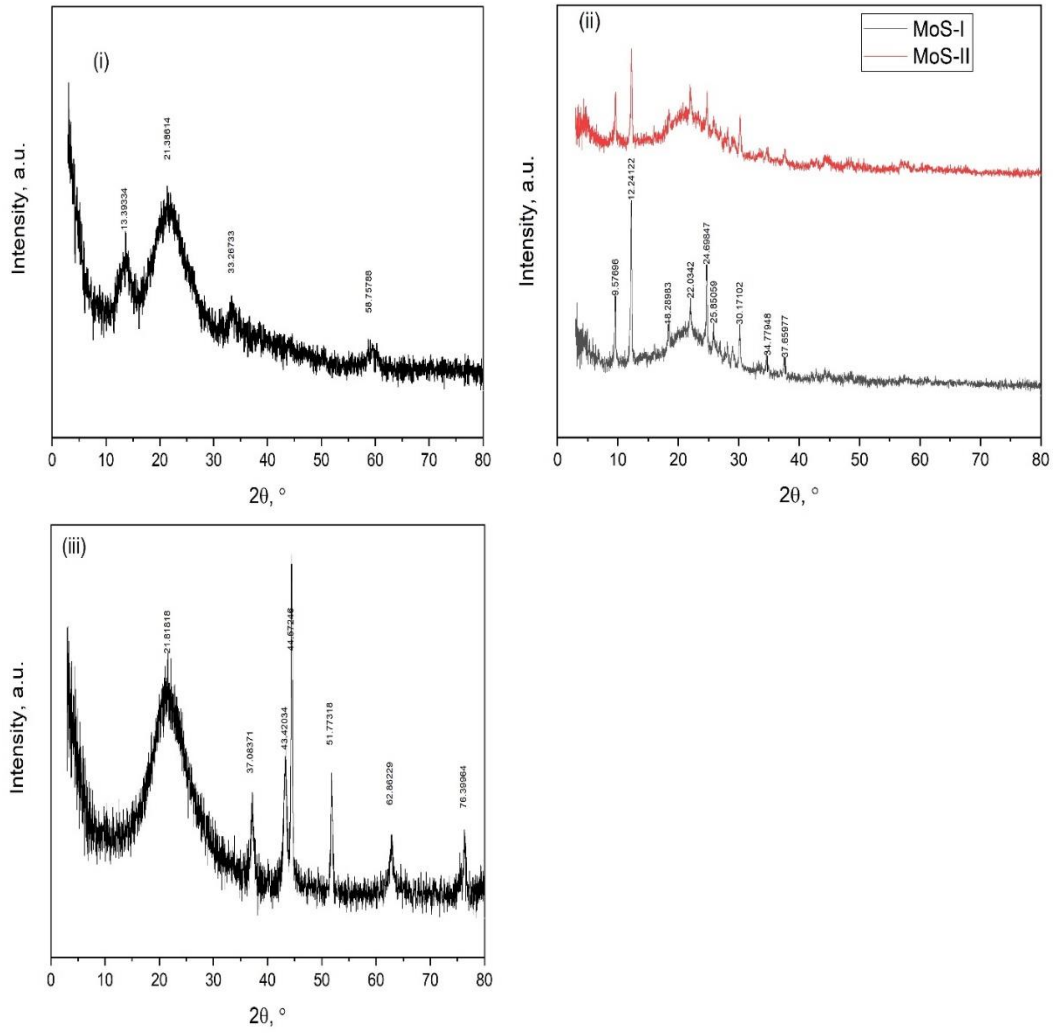

Figure 2.2: *XRD spectra of synthesized catalysts (i) CoMoS Slurry, (ii) MoS-I and MoS-II, and (iii) NiC.*

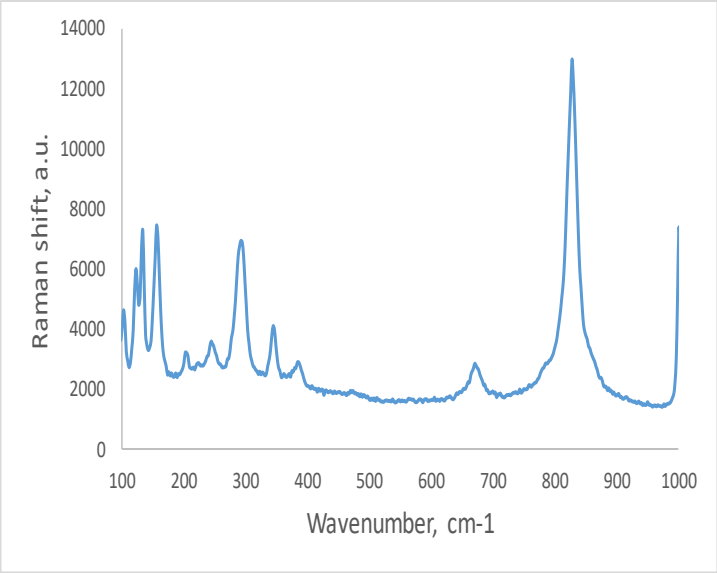

***Figure 2.3**: Raman spectrum of MoS-II catalyst.*

The surface morphology, chemical composition, and orientation of synthesized CoMoS, MoS-II, and MoS-OS slurry catalysts that were revealed by SEM are shown in Figures 2.4, 2.5, and 2.6, respectively. In Fig. 2.5, the MoS-II catalysts synthesized by the hydrothermal route are nano-flowers, assembled by lamellar nano-sheets (Fig. 2.5(iii)). The results are similar to that reported in the literature [29]. For MoS-OS (Fig. 2.6) and CoMoS slurry (Fig. 2.4) catalysts, various grains were observed, but the majority of both catalysts did not have well-defined shapes. The shape of the grains was irregular. Additionally, the SEM image shows the formation of nanostructures with agglomerates to form clusters. A few rod-like structures were also observed in these SEM images. This rod formation may be due to the presence of some oxide structures.

TEM was used for imaging and analytical characterization to assess the shape, size, and morphology. Fig. 2.7(i) shows the TEM images of the MoS-OS catalyst. It was observed that monolayered particles were formed in the Mo-based catalyst. TEM images confirmed that the well dispersed MoS_2 single slabs of a very small size were formed in the oil-soluble MoS_2 catalyst.

TEM images of the CoMoS slurry catalyst (Fig. 2.7(ii)) showed the presence of several overlapped fringe characteristics of highly disordered structures. The fringes located at the edges are very short compared to the elongated one present in the center. This difference is due to the presence of Co in the MoS_2 structure that was reported to cause a decrease in sheet lengths and an increase of stack layers [30].

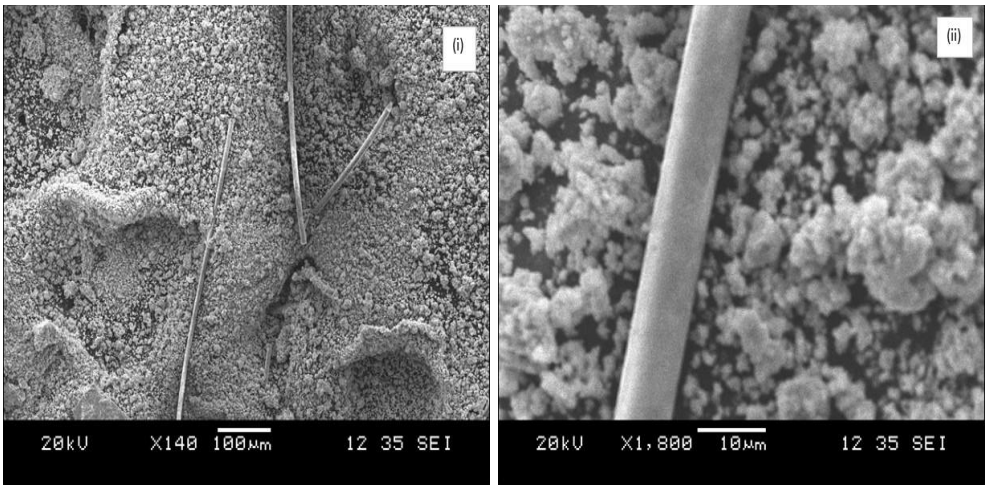

Figure 2.4*: SEM images of CoMoS-Slurry catalyst.*

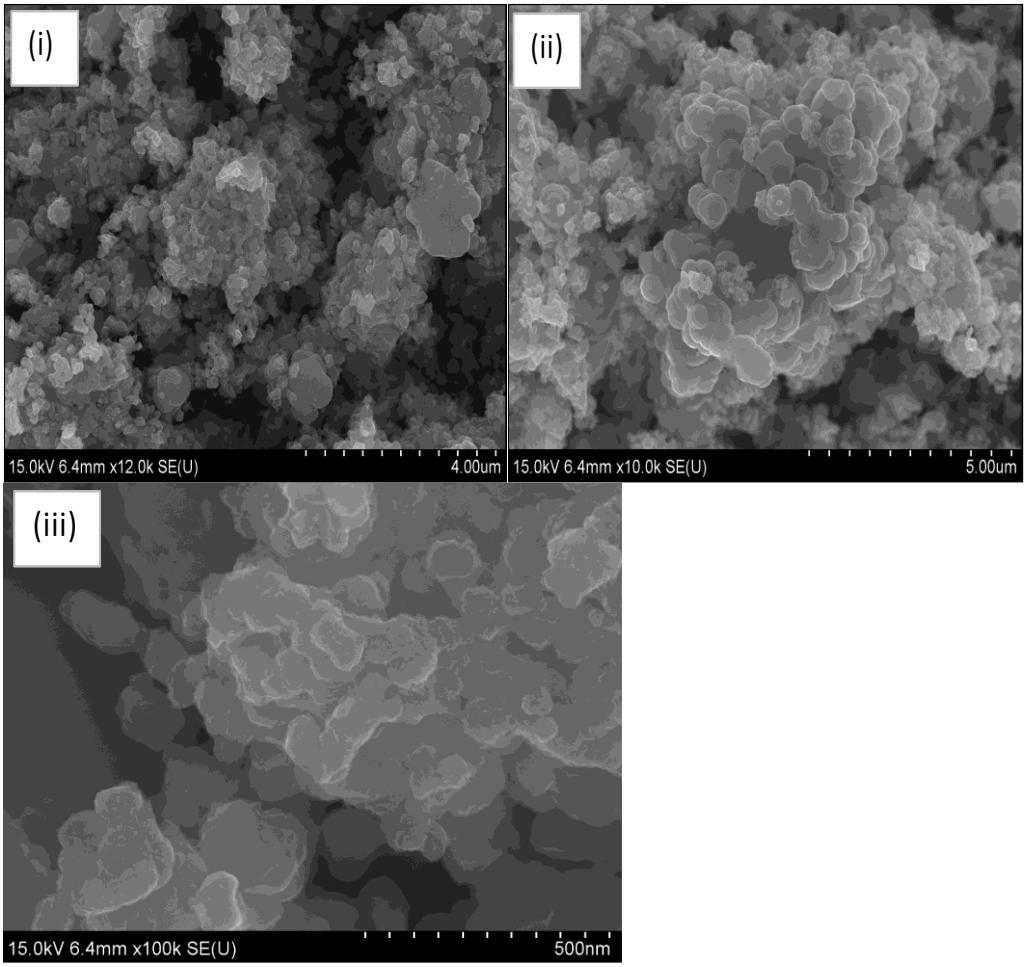

Figure 2.5*: SEM images of MoS-II catalyst.*

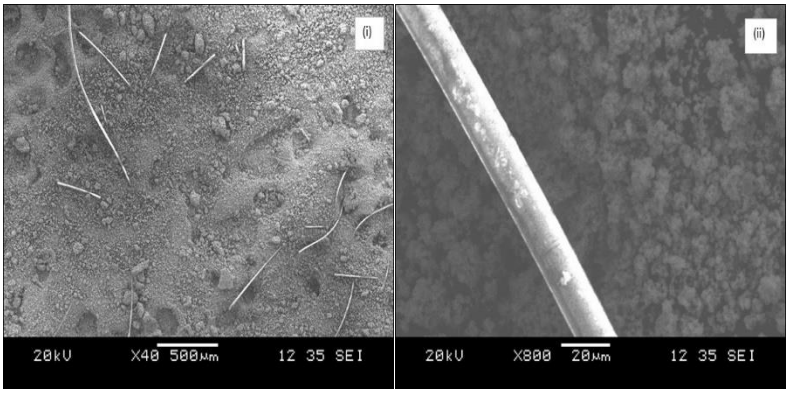

***Figure 2.6**: SEM images of MoS-OS catalyst.*

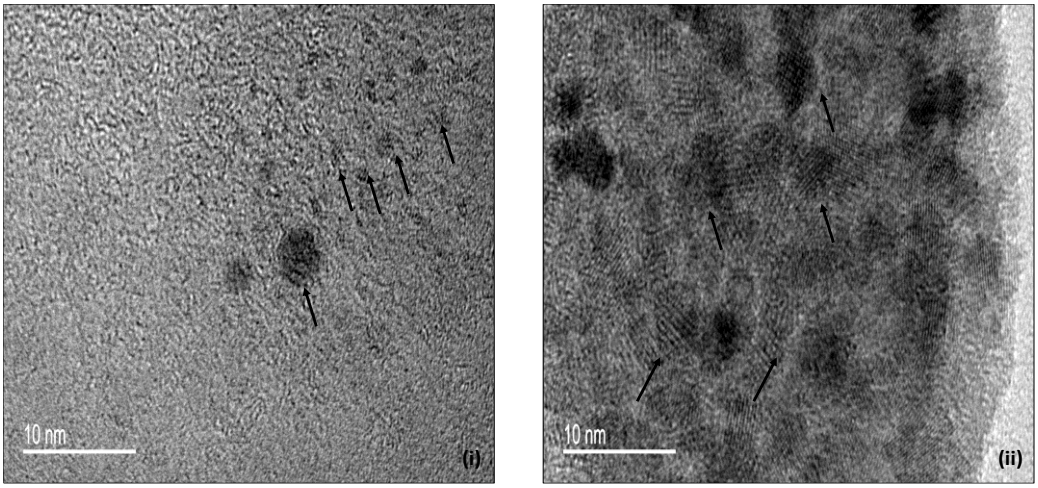

***Figure 2.7:** TEM images of (i) MoS-OS and (ii) CoMoS-Slurry catalysts. Black arrow shows the presence of MoS_2.*

2.4 Conclusions

In this work, different types of slurry phase dispersed catalysts were successfully synthesized using various synthesis procedures. Based on the characterization results of the synthesized catalysts, the following conclusions were drawn:

- The hydrothermal route is good to use for the synthesis of MoS_2 and bimetallic sulfide (CoMoS) catalysts in the nanoparticles phase and is desirable for the hydrotreating experiments.
- Oil-soluble slurry phase catalysts can be synthesized using simple precursor salts, such as ammonium heptamolybdate as a Mo source and thiourea as a sulfur source.
- A nickel carbide catalyst can be obtained from the thermolysis of nickel acetylacetonate in oleylamine.

Chapter 3: Upgradation

3.1 Sources of Biocrude Oils

Two different kinds of biocrude oils were obtained from fast pyrolysis (PBCr) and the hydrothermal liquefaction process (HTBCr). For the initial experimental runs and to set up the reactor system, a wood pellets pyrolysis biocrude oil (PBCr-I) was used [31]. Then, another low-ash, fast pyrolysis biocrude oil was purchased from the Mainstream Bioenergy Corporation (PBCr-II). The PBCr-II was produced from the fast pyrolysis of pine sawdust. The HTBCr biocrude oil was obtained from the hydrothermal treatment of a food processing waste.

3.2 Characterization Techniques

The elemental composition of the biocrude oils and the upgraded products were analyzed with a Perkin Elmer 2440, Series II CHN analyzer. All samples were analyzed twice, and the average values were reported. The amount of oxygen was determined by the difference from the total of 100. The hydrodeoxygenation (HDO) activity was calculated as:

$$HDO, \% = \frac{oxygen\ wt\%\ in\ feed - oxygen\ wt\%\ in\ product}{oxygen\ wt\%\ in\ feed} \times 100$$

The higher heating values (HHV, MJ/kg) of the feedstock and upgraded products were calculated using Dulong's formula:

$$HHV, MJ/kg = 0.0338 \times C + 1.428(H - \frac{O}{8})$$

The ash content in the biocrude oils was determined as per the American Society for Testing and Materials (ASTM) D482-13 method. Biocrude oils and the products obtained after the upgradation were analyzed using thermogravimetric analysis (TGA) to monitor weight loss as a function of temperature. TGA analysis was carried out in a Q50 TGA from TA Instruments based on the National Renewable Energy Laboratory (NREL) method for the boiling point distribution of biocrude oils [32]. In the TGA experiment, 8-10 mg of sample were loaded in a ceramic crucible and heated to 700 °C at a rate of 50 °C/min in a nitrogen atmosphere to observe the weight loss of samples as the temperature increased. After reaching 700 °C, the nitrogen atmosphere was replaced with air, and the sample was heated to 750 °C at 50 °C/min to determine the ash content of the sample. At 700 and 750 °C, the sample was held at a constant temperature for 5 min. To determine the Fourier Transform infrared (FTIR) spectra, a Thermo Nicolet Nexus 670 FTIR equipped with a single-bounce diamond attenuated total reflectance (ATR) accessory (Specac Golden Gate) and KBr beam slitter were used. Spectra were collected in the range of 4000-600 cm^{-1} with a 4 cm^{-1} resolution, and the data were processed using Omnic software. The spectra were collected after smearing the sample directly on the ATR crystal surface.

The biocrude oils and upgraded bio-oil samples were analyzed by GC-MS (Shimadzu GC-MS-QP2010SE instrument). A 10 wt% of biocrude oil sample in dichloromethane (DCM) was prepared for this analysis. The split ratio of 100:1 was used. The products were separated on an Rtx-5MS column (30 m length, 0.25 µm diameter, and 0.25 µm thickness) using a temperature program of 40 °C (held for 4 min) to 320 °C (held for 10 min) at 10 °C/min and a constant column head pressure of 0.207 MPa. The ion source was at 250 °C, and the interface temperature was 325 °C with a scan rate of 1 s over m/z 35-650. The National Institute of Standards and Technology (NIST) Standard Reference Data library was used to identify and analyze the peaks, providing information about the compounds present in the samples. The pH of the products was determined using a Beckman pH meter. Before analysis, the pH meter was calibrated using the standard pH of 2, 4, 7, and 10.

3.3 Methodology

3.3.1 Experiments Performed in a Parr Batch Reactor

The aim of the experiments planned for the batch reactor studies was to record the temperature-pressure profiles. The batch reactor experiments were performed in a Parr reactor (Model 4575A, Parr Instruments, IL, US). The reactor had a volume of 450 mL and a maximum working pressure of 3000 psi. The temperature was controlled using a proportional-integral-derivative (PID) controller (Model 4848, Parr Instruments, IL, US). The reactor was stirred continuously and heated to the desired reaction temperature. Prior to the experiments, the reactor was purged twice with nitrogen and hydrogen. The final hydrogen pressure required for the experiment was 1300 psi. Therefore, there was a need to optimize the initial pressure as per the desired reaction temperature. Keeping this in mind, few blank reactions were performed. The reactant and reaction conditions used are reported in Table 3.1.

The heating rate of the reactor was approximately 5–7 °C/min. Once the operating temperature was reached, the temperature was held for the desired reaction time. Upon completion of the reaction, the reactor was cooled using a cooling line present inside the reactor. Once the temperature reached room temperature or 25 °C, the final gas pressure and temperature were recorded and vented. The reactor was purged with nitrogen before opening. The solid and liquid products were recovered with DCM. After that, the liquids and solids were separated using vacuum filtration. The solid product was washed by DCM to extract the liquid product. The DCM soluble and aqueous fractions from the liquid product were extracted using a separating funnel. Later, excess DCM and water were evaporated. The solid product was dried in an oven at 110 °C for 30 min. The final weights of the products (DCM soluble fraction, aqueous fraction, and solid) were recorded. The samples were kept in screw-cap glass vials, labeled, and stored in a sliding-door fridge at 4 ^{o}C. The total mass balance of the product obtained was calculated.

From the experiments carried out as reported in Table 3.1, it was observed that at a 200 °C reaction temperature, a very high amount of solid coke was produced from the pyrolysis oils (i.e., PBCr-I and PBCr-II). On the other hand, with HTBCr, only viscous liquid was obtained. Another set of experiments (test runs 6–8) were planned using dispersed solid catalysts (commercially

available) at a low temperature. The reaction conditions for these experiments are given in Table 3.2.

Table 3.1: *Reaction conditions used for test run 1–5 (without catalyst) performed in a batch reactor.*

Run	Biocrude oil used, g	T,˚C	Final P, psi	Initial P, psi	Stirring rate, RPM	Time, min	Product recovered, g
Test-1	PBCr-I, 40g	170	746	420	150	120	34
Test-2	PBCr-I, 28g	200	640	450	150	120	24
Test-3	HTBCr, 50g	200	643	420	150	120	50 (some DCM)
Test-4	PBCr-II, 52g	200	700	420	150	120	49
Test-5	PBCr-II, 50g	170	570	412	150	120	47

Table 3.2: *Reaction conditions used for the upgradation of PBCr-II (experiments conducted in a batch reactor).*

Run	Biocrude oil, g	Catalyst, g	T,˚C	Final P, psi	Initial P, psi	Stirring rate, RPM	Time, min	Product recovered, g
Test-6	50	PMA+Tetralin, 0.2038+4-5ml	180	761	520	150	120	53 (some DCM)
Test-7	50	Pt/C, 0.5g	190	1101-959	760	170	120	45
Test-8	51	Ni/C, 1g	190	1131-843	760	150	120	49

PMA=phosphomolybdic acid; Pt/C=platinum supported on carbon; and Ni/C=synthesized using activate carbon support.

In test runs 6–8, a sticky solid product formed. This product was not soluble in DCM. Therefore, another method was performed for product separation. In this case, tetrahydrofuran (THF) was used to dissolve and remove the product from the vessel. To test the feasibility of the separation process, two methods were used: soxhlet extraction and vacuum filtration using THF. From these results, we decided to use the THF vacuum filtration route to separate the two fractions (i.e., THF soluble and THF insoluble).

3.3.2 Experiments Performed in a Microwave Reactor

The biocrude oil upgradation using PBCr-II was also screened in a microwave reactor (Biotage® Initiator+) with ethanol as a solvent. The biocrude oil (1.0 g) with the ethanol (2 mL) was loaded into microwave vials (5 mL). The reaction conditions used are reported in Table 3.3.

Table 3.3: *PBCr-II upgradation in a microwave reactor using ethanol as solvent.*

Sample	Reaction condition	pH
PBCr-II+EtOH (2 mL)	Room temperature	3.43
PBCr-II+EtOH (2 mL)	160°C, 30 min, 1 MPa	3.61
PBCr-II+EtOH (2 mL)	170°C, 60 min, 1.3 MPa	3.49
PBCr-II+EtOH (2 mL)	180°C, 60 min, 1.8 MPa	3.45
PBCr-II+EtOH (2 mL) + Amberlyst Catalyst	170°C, 30 min, 1.5 MPa	2.50

3.3.3 Experiments Performed in 10 mL Autoclave Reactor Tubes

For these experiments, an autoclave reactor tube was prepared and packed with 1 g of biocrude oil along with a desired amount of catalyst. The reactor tube was stirred on a shaker at 700 RPM at 40 °C for 30 min. The reactor tube was tightened and checked for leakage using nitrogen. The reactor was pressurized to 653 psi of hydrogen pressure. The reactor tube was then placed in a preheated furnace at 350 °C. The temperature during the reaction was recorded using a digital thermometer attached to a reactor tube. Approximately 40 min was required for the reactor tube to reach the desired reaction temperature of 350 °C. Then, the reaction was performed for 2 h. After reaction completion, the reactor tube was immediately removed from the furnace and immersed in water. After cooling the reactor tube to room temperature, the pressure was recorded using a pressure gauge. The products obtained were recovered with DCM and vacuum filtered to separate the liquid and solid fractions. The DCM was evaporated from the liquid product and final weights were recorded. The solid product was dried at 110 °C for 80 min to calculate the solid percentage after removing the amount of fresh catalyst added initially in the reactor from the dry weight. The total mass balance calculations were performed, and the samples were transferred to screw-cap glass vials and stored in a sliding-door fridge at 4 ^{o}C for further analysis. The liquid and solid yields were calculated as:

$$Liquid\ \% = \frac{amount\ of\ liquid\ recovered\ after\ DCM\ evaporation}{amount\ of\ biocrude\ oil\ used} \times 100$$

$$Solid\ \% = \frac{(amount\ of\ solid\ recovered - amount\ of\ catalyst\ used)}{amount\ of\ biocrude\ oil\ used} \times 100$$

3.4 Results and Discussion

3.4.1 Biocrude Oil Characterization

Table 3.4 summarizes some typical properties of the biocrude oils used for this study. The oxygen content in the pyrolysis biocrude oils (34.81 wt% for PBCr-I and 40.8 wt% for PBCr-II) was higher than in the HTBCr biocrude oil (11.71 wt%). Because of its low oxygen content, HTBCr biocrude oil had the highest HHV (higher heating value) of 40 MJ/kg.

3.4.1.1 TGA Analysis

The TG curve provides the weight loss curve as a function of temperature. It also gives information on the volatility of the biocrude oils and allows for the evaluation of the carbon residue. Fig. 3.1 shows the weight loss curves from the TGA analysis of the biocrude oils. The results showed that about 14.11 wt% of the HTBCr biocrude oil was evaporated at 250 °C. The TG curve showed that the HTBCr biocrude oil contained more high boiling compounds compared to pyrolysis biocrude oils (PBCr-I and PBCr-II). From the DTG curve in Fig. 3.1 (iii), three marked peaks are visible, which might be due to three different compound types present in the HTBCr biocrude oil.

3.4.1.2 FT-IR Analysis

The FT-IR analysis of biocrude oils provides information about the functional group characteristics. Fig. 3.2 presents the FT-IR analysis of PBCr-II and HTBCr.

In the IR spectra of PBCr-II, the following characteristics were observed:

- Strong IR absorbance associated with the O-H group stretch (3333 cm^{-1});
- Weak C-H stretch associated with various saturated and unsaturated aliphatic and aromatic compounds (2800–3000 cm^{-1});
- Characteristic C=O stretch of aldehydes, ketones, and acids (1600–1700 cm^{-1});
- Aromatic C=C (1500–1600 cm^{-1}); and
- Fingerprint region below 1500 cm^{-1}.

Sharp peaks were observed in the HTBCr biocrude oil compared to PBCr-II. Also, in the IR spectra of HTBCr, the following characteristics were observed:

- Prominent C-H stretch (3000–2840 cm^{-1});
- CH_2 bending (1465 cm^{-1});
- CH_3 bending (1375 cm^{-1});
- Strong acid and ester peaks (1700 cm^{-1}); and
- Strong peak around 720 cm^{-1} along with strong C-H stretching peak (3000–2840 cm^{-1}), indicative of long-chain alkyls.

Table 3.4: *Characteristics of the biocrude oils used.*

Properties	**PBCr-I**	**PBCr-II**	**HTBCr**
Ash content, wt%	4.472	0.0064	0.3652
Water content, wt%*	-	29.3	-
C, wt%	58.58	52.25	76.73
H, wt%	6.51	6.78	11.31
N, wt%	0.003	0.18	0.26
S, wt%	0.007	0.02	-
O, wt%	34.81	40.80	11.71
HHV, MJ/kg	22.89	22.19	40

*water content of PBCr-II was provided by Mainstream Bioenergy Corporation

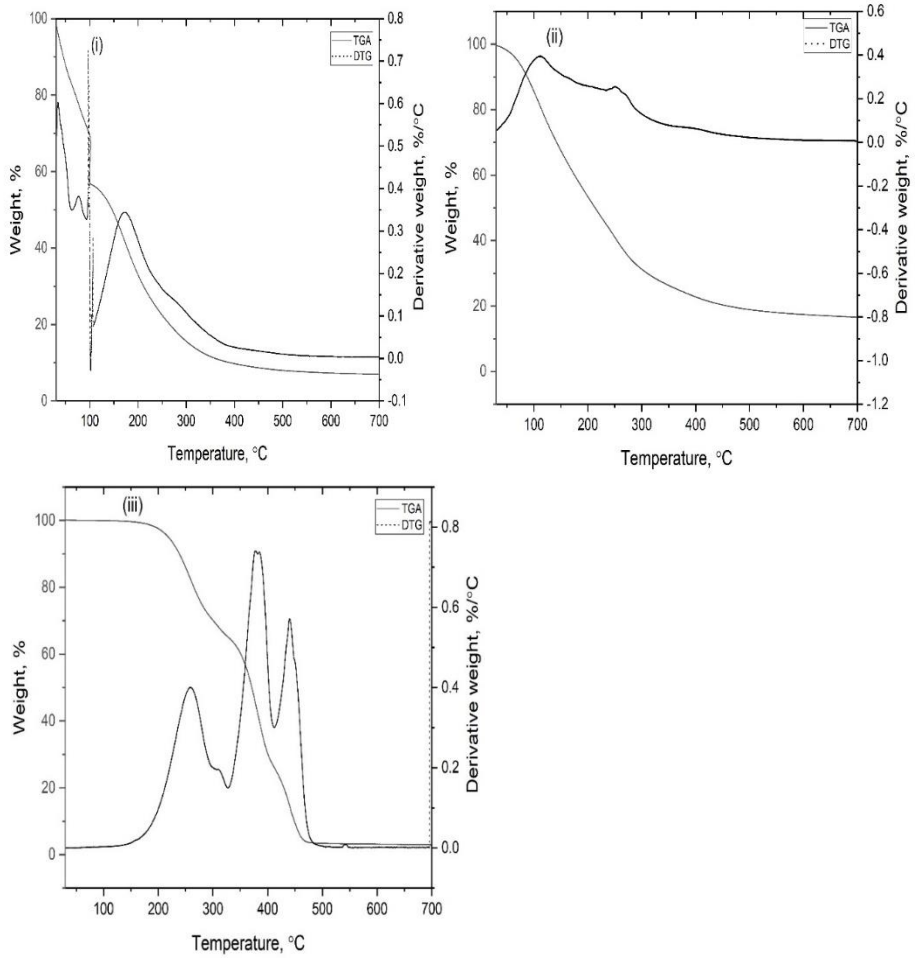

Figure 3.1: *TGA curves of the biocrude oils (i) PBCr-I, (ii) PBCr-II, and (iii) HTBCr.*

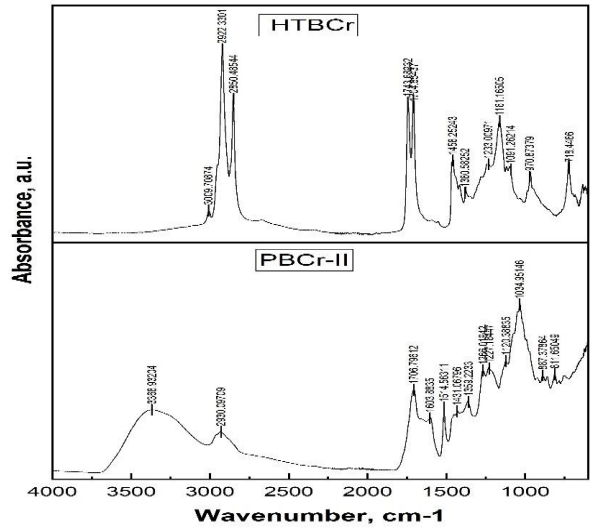

Figure 3.2: *FT-IR spectra of the biocrude oils.*

3.4.1.3 GC-MS Analysis

The chemical compounds present in the biocrude oils affect their overall usefulness; therefore, their identification is necessary. Tables 3.5 and 3.6 display the area percentage of various compounds identified using GC-MS for PBCr-II and HTBCr, respectively. It is well known that the GC-MS measurements capture only a small portion of the chemical identities present in biocrude oils, and there exists undetectable compounds of larger molecular weight and boiling points due to the temperature limit of the instrument (maximum boiling point detected ~350 °C).

The PBCr-II contains a wide range of compounds such as phenolic compounds (alcohols), aldehydes, ketones, acids, and amines. The most prevalent peak in alcohols was for cresol (~11%), phenol (2.8%), and phenol derivatives, such as phenol-2-methoxy-3-(2-propenyl) (4.6%) and phenol-3-methyl (1.63%). The aldehydes included succindialdehyde (1.44%), furfural (1.98%), pentanal (4.18%), 5-hydroxymethylfurfural (0.55 %), coniferyl aldehyde (3.48%), and vanillin (2.09%). Ketones were also present in PBCr-II, having a carbon number in the range of C3-C20. The amount of amines was present in a lesser quantity compared to the rest of the heteroatoms. The GC-MS analysis was in good agreement with the FT-IR spectra for PBCr-II.

In HTBCr, 40% of the compounds were detected as 11-octadecanoic acid and 25% as 9,12-octadecadienoic acid. The results showed that major compounds in this biocrude oil were fatty acid derivatives and these results agree with the reported literature [33]; the same was seen also in the FTIR spectrum.

3.4.2 Pyrolysis Biocrude Oil (PBCr-II) Upgrading

Microwave experiments: The objective in performing the reaction in a microwave reactor was to check whether esterification of the pyrolysis biocrude oil could be achieved this way. It was expected that after the reaction the pH of these biocrude oils would increase. The pH of the products is also reported in Table 3.3. A negligible increase in pH was observed at 160 °C compared to PBCr-II+EtOH at room temperature. However, in the presence of an Amberlyst catalyst, the pH decreased to 2.50. These results were not promising; this methodology needs to be explored further with other, more suitable, catalysts.

Parr reactor experiments: As explained in Section 3.3.1, pyrolysis of biocrude oils produces a solid, sticky product in the absence of any catalyst in the test runs performed in the batch reactor. Therefore, to move forward with the catalytic runs, first a process needed to be developed for upgrading the pyrolysis biocrude oils. With this main goal, a few more experimental runs were conducted.

Table 3.5: *GC-MS analysis of PBCr-II.*

	RT, min	Compound Name	Chemical Formula	Area, %
Alcohols				
	2.08	2-amino-1,3-propanediol	$C_3H_9NO_2$	1.58
	9.78	Phenol	C_6H_6O	2.79
	11.18	Phenol, 2-methyl-	C_7H_8O	0.81
	11.55	Phenol, 3-methyl-	$C_7H_8O_2$	1.63
	11.80	Phenol, 2-methoxy-	$C_7H_8O_2$	0.84
	12.80	Phenol, 2,5-dimethyl-	$C_8H_{10}O$	0.5
	13.51	Creosol	$C_8H_{10}O_2$	10.56
	14.47	1,2-benzenediol, 4-methyl-	$C_7H_8O_2$	1.61
	14.80	Phenol, 4-ethyl-2-methoxy-	$C_9H_{12}O_2$	3.74
	14.89	1,2-benzenediol, 4-methyl-	$C_7H_8O_2$	2.32
	15.33	2-methoxy-4-vinylphenol	$C_9H_{10}O_2$	1.91
	15.91	Phenol, 2-methoxy-3-(2-propenyl)	$C_{10}H_{12}O_2$	4.63
	16.05	Phenol, 2-methoxy-4-propyl-	$C_{10}H_{14}O_2$	1.01
	16.61	Phenol, 2-methoxy-4-(1-propenyl)-, (Z)-	$C_{10}H_{12}O_2$	1.73
	17.19	trans-Isoeugenol	$C_{10}H_{12}O_2$	6.57
	17.25	Phenol, 2-methoxy-4-propyl-	$C_{10}H_{14}O_2$	0.9
	19.58	Benzenepropanol, 4-hydroxy-3-methoxy-	$C_{10}H_{14}O_3$	2.41
	18.72	4-(1-Hydroxyallyl)-2-methoxyphenol	$C_{10}H_{12}O_3$	1.19
Aldehydes				
	5.25	Succindialdehyde	$C_4H_6O_2$	1.44
	6.53	Furfural	$C_5H_4O_2$	1.98
	11.90	Pentanal	$C_5H_{10}O$	4.18
	13.97	5-hydroxymethylfurfural	$C_6H_6O_3$	0.55
	20.59	Coniferyl aldehyde	$C_{10}H_{10}O_3$	3.48
	16.50	Vanillin	$C_8H_8O_3$	2.09
Ketones				
	2.85	2-propanone	$C_3H_6O_2$	4.71
	5.01	2-propanone, 1-hydroxy	$C_3H_6O_2$	1.97
	7.11	2-heptanone, 3-methyl-	$C_8H_{16}O$	1.59
	7.38	2-propanone, 1-(acetyloxy)-	$C_5H_8O_3$	0.64
	8.26	2(5H)-furanone	$C_4H_4O_2$	1.95
	8.61	1,2-cyclopentanedione	$C_5H_6O_2$	1.71
	9.47	2-cyclopenten-1-one, 3-methyl-	C_6H_8O	2.14
	9.65	2(5H)-furanone, 3-methyl-	$C_5H_6O_2$	0.45
	10.64	1,2-cyclopentanedione, 3-methyl-	$C_6H_8O_2$	2.15
	10.93	4-methyl-5H-furan-2-one	$C_5H_6O_2$	0.62
	17.64	Ethanone, 1-(3-hydroxy-4-methoxyphenyl)-	$C_9H_{10}O_3$	3.66
	18.14	2-propanone, 1-(4-hydroxy-3-methoxyphenyl)-	$C_{10}H_{12}O_3$	1.56
	29.02	Dibenz[d,f]cycloheptanone, 2,3,9-trimethoxy-	$C_{18}H_{18}O_4$	3.87
	30.79	3,4-Divanillyltetrahydrofuran	$C_{20}H_{24}O_5$	1.72
Acids				
	2.20	Acetic acid	$C_2H_4O_2$	3.29
	19.30	Butanedioic acid, methyl-	$C_5H_8O_4$	1.28
	27.32	Dehydroabietic acid	$C_{20}H_{28}O_2$	1.95
	29.51	1,3-Benzenedicarboxylic acid, bis(2-ethylhexyl) ester	$C_{24}H_{38}O_4$	1.12
Amines				
	10.18	N,N-diamylmethylamine	$C_{11}H_{25}N$	0.55
	18.31	1-nitro-.beta.-d-arabinofuranose, tetraacetate	$C_{13}H_{17}NO$	2.62

Table 3.6: *GC-MS analysis of HTBCr.*

RT, min	Compound Name	Chemical Formula	Area, %
22.92	n-hexadecanoic acid	$C_{16}H_{32}O_2$	7.49
23.24	Hexadecanoic acid, ethyl ester	$C_{18}H_{36}O_2$	1.36
24.61	9,12-octadecadienoic acid (Z,Z)	$C_{18}H_{32}O_2$	24.86
24.71	17-octadecynoic acid	$C_{18}H_{32}O_2$	14.7
24.83	9,12-octadecadienoic acid (Z,Z)-	$C_{18}H_{32}O_2$	5.16
24.88	(E)-9-octadecenoic acid ethyl ester	$C_{20}H_{38}O_2$	3.87
24.94	9,12-octadecadienoic acid (Z,Z)	$C_{18}H_{32}O_2$	2.28
24.68	11-octadecanoic acid	$C_{18}H_{34}O_2$	40.28

Based on the literature reports [34–36] for the upgradation of pyrolysis biocrude oils, the PBCr-II upgradation was performed using water and methanol as a reaction medium. First, for these experimental runs, a test was conducted in the Parr batch reactor to get the temperature-pressure profile (given in Table 3.7). With no initial pressure, the maximum pressure reached was 880 psi at 300–320 °C. Therefore, the same set of experiments was planned in small reactor tubes (10 mL) at different temperatures (300–350 °C). The results are shown in Fig. 3.3.

The upgradation of PBCr-II biocrude oil using water and methanol reaction media leads to the production of 35–40% solids. The amounts of solid produced were very high; therefore, further upgradation experiments were performed directly with catalysts in the 10 mL reactor tubes. These results are presented in Fig. 3.4.

The results revealed that in a blank reaction (non-catalytic), 55.6% solids and 43.4% liquids were produced. Gas samples were not analyzed as it was outside the scope of this project. The evaluation of the catalyst activities showed that the amounts of solids produced in the catalytic experiments were less compared to those of the blank run. The amounts of solids produced with CoMoS Cmr and CoMoS slurry catalysts were 41% and 29%, respectively. It is clear that the CoMoS slurry catalyst showed a lesser amount of coke formation and more liquid production. The NiS slurry catalyst also showed the formation of 29% solids and 64% liquids. For the MoC catalyst test run, 500 wppm of the metal was used and 38% solids was produced. This difference is due to the lower amount of catalyst used compared to the other catalytic runs.

Another set of experiments was conducted using carbide-based dispersed catalysts. The amounts of solid and liquid products are given in Fig. 3.5. The amounts of liquid products obtained with NiC, MoC, and NiMoC were somewhat higher compared to the blank run. A repeat run with the MoC catalyst (MoC-re) showed that the solid products were still higher (35–38%) than the other catalysts, but lower compared to the blank run (56%). An experimental run using AHM showed results similar to the other catalysts in terms of solid production.

3.4.2.1 CHNO Analysis

Properties of the liquid products are reported in Table 3.8. HDO conversions reported with a blank, MoC, NiC, and NiMoC were 53%, 56%, 55%, and 53%, respectively. HHV values of the liquid products also increased proportionately compared with the feedstock. Further reaction optimization studies are required to achieve a desirable product quality. This includes optimization of reaction temperature, reaction time, and catalyst amount to maximize product yield and quality with pyrolysis biocrude oil.

Table 3.7: *Profile for temperature and pressure for the PBCr-II recorded from Parr reactor test. [Feed: PBCr-II (10 g), methanol (13 ml); water (10 ml)].*

Time	Set T, °C	Actual T, °C	Pressure, psi	RPM	Heater	Remarks
10:30	50	11	0	302	I	
10:36	70	14				
10:50	110	72	0	302		
10:57	150	105	0	303		
11:10	180	129	018	303		
11:15	180	150	066	303		
11:35	200	177	169	304	II	
11:41	250	198	256			
11:51	250	243	579			
11:59	250	249	636			250 °C, Stayed 15min 636-625psi
12:03	250	244	605			
12:06	250	247	621			
12:15	250	246	625			
12:15	280	246	628			
12:18	280	250	658			
12:26	280	270	776			
12:30	290	298	817			
12:37	290	293	816			
12:46	300	295	819			300 °C, stayed 45min 827-831psi
12:46	300	296	827			
12:46	300	297	829			
12:55	300	299	837			
1:30	310	297	831			
1:30	310	296	828			
1:50	320	306	853			On gauge 850psi
1:50	320	306	853			
2:05	320	318	879			
2:20	320	316	873			
2:50	320	317	861			
3:26	320	318	848			
3:32	50	168	77			
		151	46			

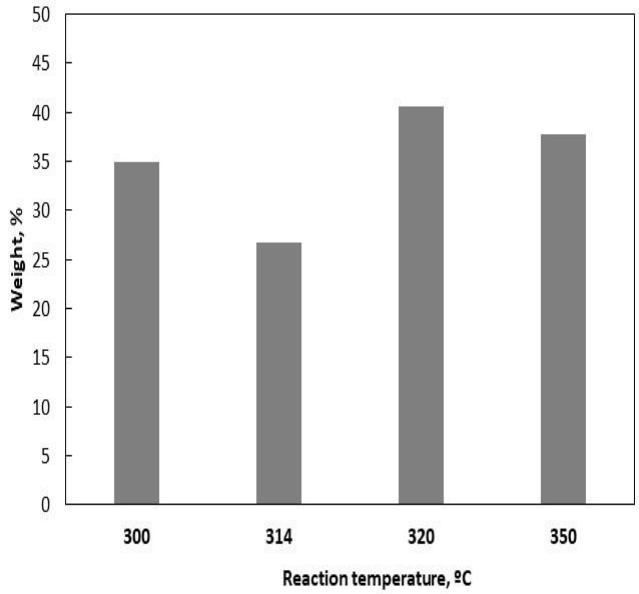

Figure 3.3: *The amount of solid product obtained after the PBCr-II upgrading using water and methanol as a reaction medium.*

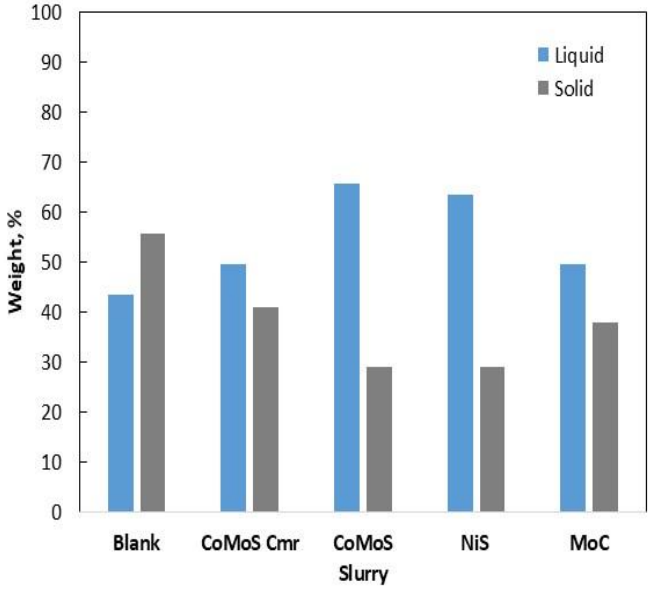

Figure 3.4: *The amount of solid and liquid products obtained after the PBCr-II upgrading using different synthesized catalysts. [Reaction conditions: T=350 °C, P=653 psi (initial), t=2 h, catalyst amount=20 wt% of CoMoS (Cmr), 2.5 wt% NiS, 2.5 wt% CoMoS slurry, and 0.59 wt% MoC (500 wppm of Mo-metal)].*

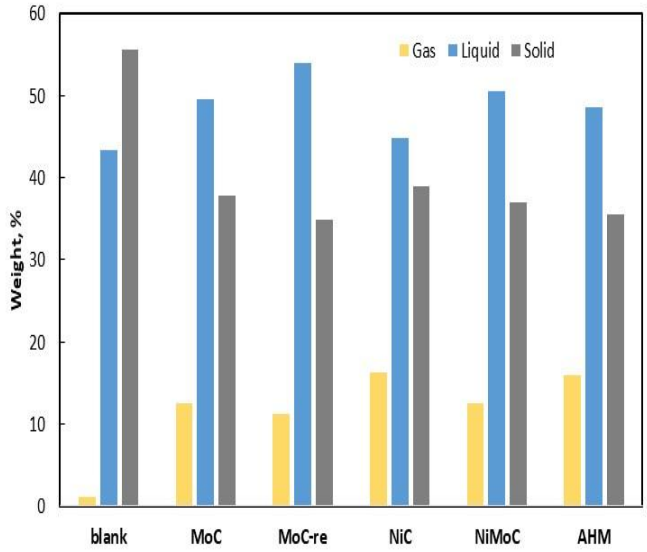

Figure 3.5: *The amount of solid and liquid products obtained after the PBCr-II upgrading using different carbide-based slurry catalysts and AHM. [Reaction conditions: T=350 °C, P=653 psi (initial), t=2 h, catalyst amount=0.57 wt% for MoC, NiC and 0.09 wt% of NiMoC].*

Table 3.8*: Properties of liquid products.*

Properties	PBCr-II	Blank	MoC	MoC-re	NiC	NiMoC
C, wt%	52.25	77.8	76.8	78.8	78.5	78.1
H, wt%	6.78	8.3	7.9	8.2	8	7.9
N, wt%	0.18	0.4	0.4	0.3	0.5	0.4
O, wt%	40.80	13.6	14.8	12.7	13.1	13.5
HDO, %	-	52.9	55.8	48.5	54.7	53.1
HHV, MJ/kg	22.19	35.6	34.7	36.1	35.6	35.3

3.4.3 Hydrothermal Liquefaction Biocrude Oil (HTBCr) Upgradation

3.4.3.1 Metal Sulfide-based Slurry Phase Dispersed Catalysts

The upgradation of HTBCr (biocrude oil obtained after the hydrothermal liquefaction of a food processing waste) was performed in a tube reactor with a 10 mL capacity. The reaction conditions used for the initial screening included a reaction temperature of 350 °C, initial hydrogen pressure of 653 psi, and a reaction time of 2 h. The catalyst amount used was 2.5 wt% of all the slurry catalysts and 20 wt% of the CoMoS Cmr catalyst. The reaction conditions were selected based on previous studies performed by our lab group as mentioned in reference [15]. The only difference from the previous study was the lesser amount of initial hydrogen pressure used in the present study. The CoMoS Cmr catalyst was the same catalyst that was used in previous investigations

[15], and it is considered a reference catalyst used to check the feasibility of slurry catalysts for the HTBCr upgradation.

The key parameter considered for these conversion studies was the minimum production of solids. Fig. 3.6 (i) presents the amount of solid and liquid products obtained after the HTBCr upgradation of CoMo Cmr and CoMoS slurry catalysts. The results were compared with a blank run (without a catalyst). The results showed that the amount of liquid product obtained with the CoMoS slurry catalyst was significantly higher compared to that of the CoMoS Cmr and the blank runs.

Additional slurry sulfide catalysts were tested for the HTBCr upgradation, and the results are shown in Fig. 3.6 (ii). From Fig. 3.6, the following conclusions were drawn:

- The mass balance based on the amount of liquids and solids was within ±5 wt%.
- All the catalysts showed good conversion activities compared to the blank run as the yield of liquid product was higher and the amount of solids was lower with all the catalysts studied.
- The amount of liquids produced with all the slurry catalysts was higher compared to that of the CoMoS Cmr catalyst.
- Among the Mo-sulfide catalysts prepared by precipitation (MoS-I) and the hydrothermal (MoS-II) route, the catalyst synthesized by the hydrothermal route showed less formation of solids. Therefore, the hydrothermal route was found to be good for the synthesis of sulfide catalysts.
- The oil-soluble molybdenum sulfide catalyst (MoS-OS) showed the highest catalytic activity in terms of production of the highest amount of liquids and the lowest amount of solids.

The repeatability of the experimental runs was performed with catalysts CoMoS slurry, MoS-I, and MoS-II. Those results are shown in Fig. 3.7. The repeat runs are designated by catalyst name followed by “re.” As shown in Fig. 3.7, the repeatability of the test runs was good. The standard deviations (SDs) for the CoMoS Slurry, MoS-I, and MoS-II catalysts were 0.19, 0.47, and 1.34 for liquid products, respectively, whereas for solid products the SDs for the CoMoS Slurry, MoS-I, and MoS-II catalysts were 0.56, 0.66, and 1.35, respectively.

3.4.3.1.1 TGA Analysis

TGA-DTG curves of the upgraded products obtained after the upgradation of HTBCr are shown in Fig. 3.8. The derivative of all the catalytic runs showed different boiling regions than in the HTBCr feed (Fig. 3.8). The weight loss at temperatures <350 °C was increased in the product obtained after the upgradation of HTBCr with an MoS-II catalyst. This means that the liquid product contained a large amount of materials in the boiling range of <350 °C.

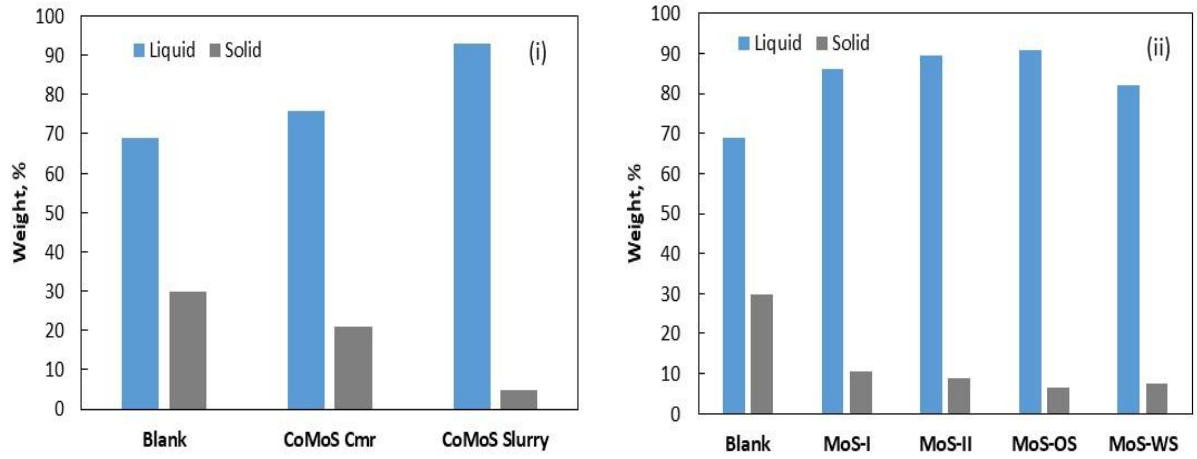

Figure 3.6: *The amount of solid and liquid products obtained after the HTBCr upgrading using different synthesized slurry catalysts (i) Comparison of slurry phase bimetallic catalyst (CoMoS Slurry) with conventional catalyst (CoMoS Cmr) and (ii) Mo-based slurry phase catalysts. [Reaction temperature 350 °C, initial hydrogen pressure 653 psi, reaction time 2 h, and catalyst amount 2.5 wt% for slurry catalysts and 20 wt% for CoMoS Cmr catalyst].*

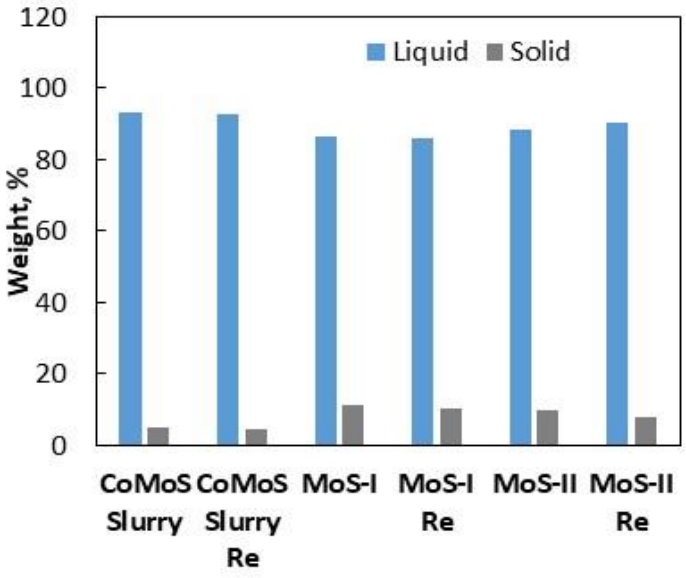

Figure 3.7: *Repeatability of the catalyst activity studies using HTBCr biocrude oil.*

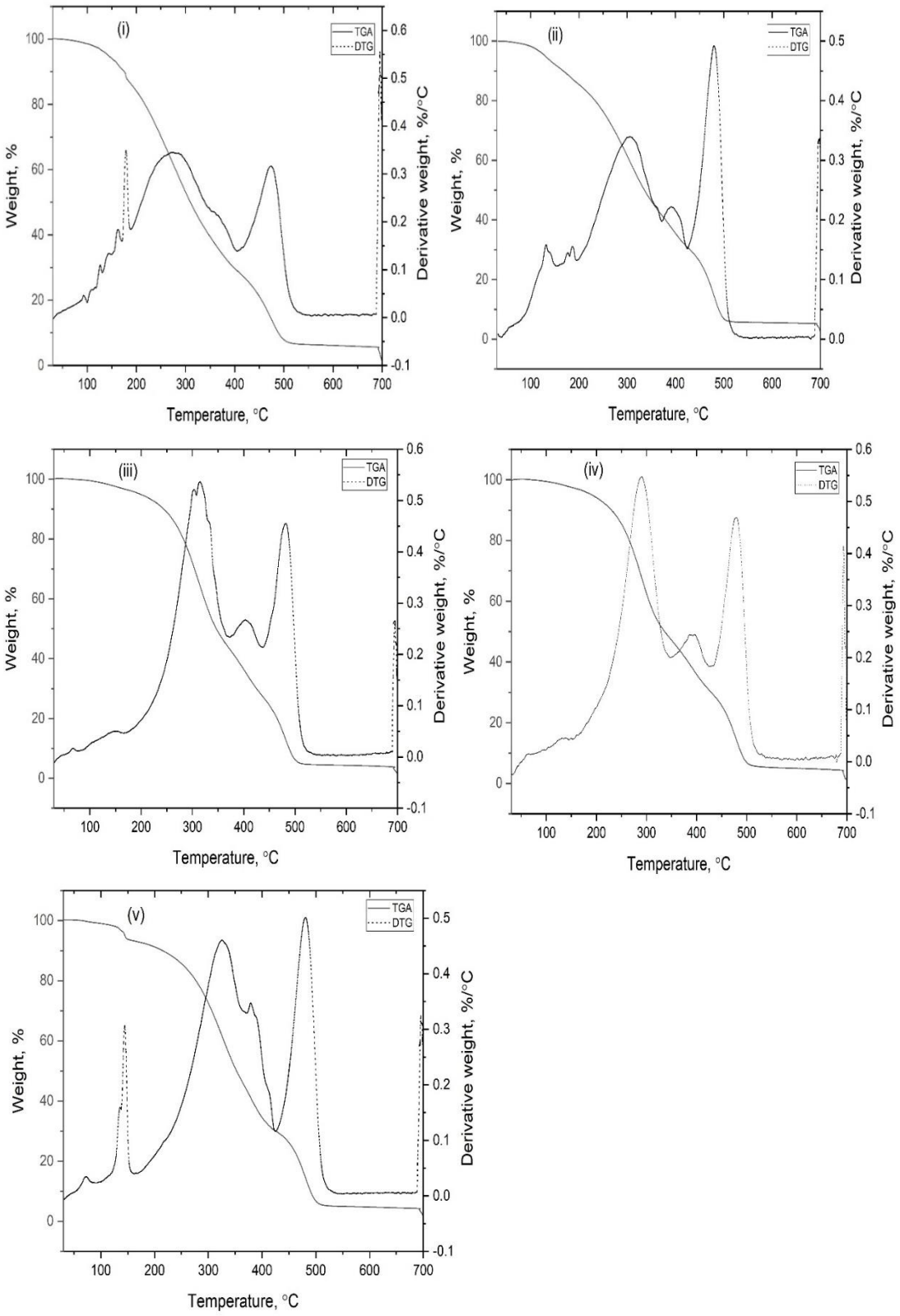

Figure 3.8: *TGA-DTG curves of products from HTBCr upgradation with (i) blank, (ii) CoMoS-Cmr, (iii) CoMoS-Slurry, (iv) MoS-I, and (v) MoS-II catalysts.*

3.4.3.1.2 CHNO Analysis

The results from the CHN analysis of the liquid products from the upgradation studies are reported in Table 3.9. To calculate the HDO activities of the studied catalysts, the oxygen content was determined by the difference (100 – (C+H+N)) and reported in Table 3.9. In the feed HTBCr and blank run (without catalysts, only hydrogen), the oxygen content was 11.71 and 11.67 wt%, respectively, which showed that no oxygen removal occurred in the presence of the hydrogen only. Therefore, a catalyst is required for better HDO activity. This expected result was observed in the experiments. When a catalyst was used, the amount of oxygen in the liquid product was reduced as compared to the blank run and feed HTBCr. The amount of oxygen content in liquid products obtained from the sulfide slurry catalysts ranged from 9 to 9.7%, except with MoS-OS. An oil-soluble molybdenum catalyst (MoS-OS) showed HDO activity similar to the commercial catalyst (CoMoS-Cmr). The rest of the catalysts showed lower HDO activity compared to other sulfide-based slurry catalysts. The reason for this result might be the large amount (2.5 wt%) of slurry catalysts used, as the typical metal concentrations used in slurry catalysis are in the ppm level. Therefore, the MoS-OS catalyst was further selected to study the slurry phase upgradation of HTBCr.

3.4.3.1.3 FT-IR Analysis

The FT-IR analysis of biocrude oil and liquid products after hydrotreatment provides information about the functional oil group characteristics. Fig. 3.9 (i) presents the FT-IR analysis of the HTBCr and the liquid products from the blank run and catalytic runs with CoMoS Cmr and CoMoS slurry catalysts. Like the elemental analysis, the high carbon and hydrogen content of HTBCr and liquid products produced prominent C-H stretch (3000-2840 cm^{-1}), CH_2 bending (1465 cm^{-1}), and CH_3 bending (1375 cm^{-1}). HTBCr showed significant peaks for heteroatom functionalities (1700-1100 cm^{-1}), and the intensity of these peaks decreased in the upgraded products. Fig. 3.9 (ii) displays the FT-spectra for the Mo-based sulfide catalysts. The differences between the spectra of the liquid products from MoS-II, MoS-OS, and MoS-WS were much less than the differences between the spectra of the CoMoS Cmr and CoMoS slurry catalysts.

Table 3.9: *CHNO results of the liquid products obtained after the HTBCr upgradation reaction.*

Properties	**HTBCr**	**Blank**	**CoMoS Cmr**	**CoMoS Slurry**	**MoS-I**	**MoS-II**	**MoS-OS**	**MoS-WS**
Ash content, wt%		1.288	2.525	1.611		1.691		
C, wt%	76.73	77.08	79.71	78.1	78.71	78.28	79.93	78.02
H, wt%	11.31	11.08	12.28	11.8	12.015	11.98	12.225	12.29
N, wt%	0.26	0.18	0.25	0.315	0.205	0.25	0.295	0.68
O, wt%	11.71	11.67	7.77	9.785	9.07	9.49	7.55	9.01
HDO, wt%	-	0.34	33.66	16.40	22.51	18.92	35.50	23.02
HHV, MJ/kg	40	39.8	43.09	41.50	42.14	41.87	43.13	42.31

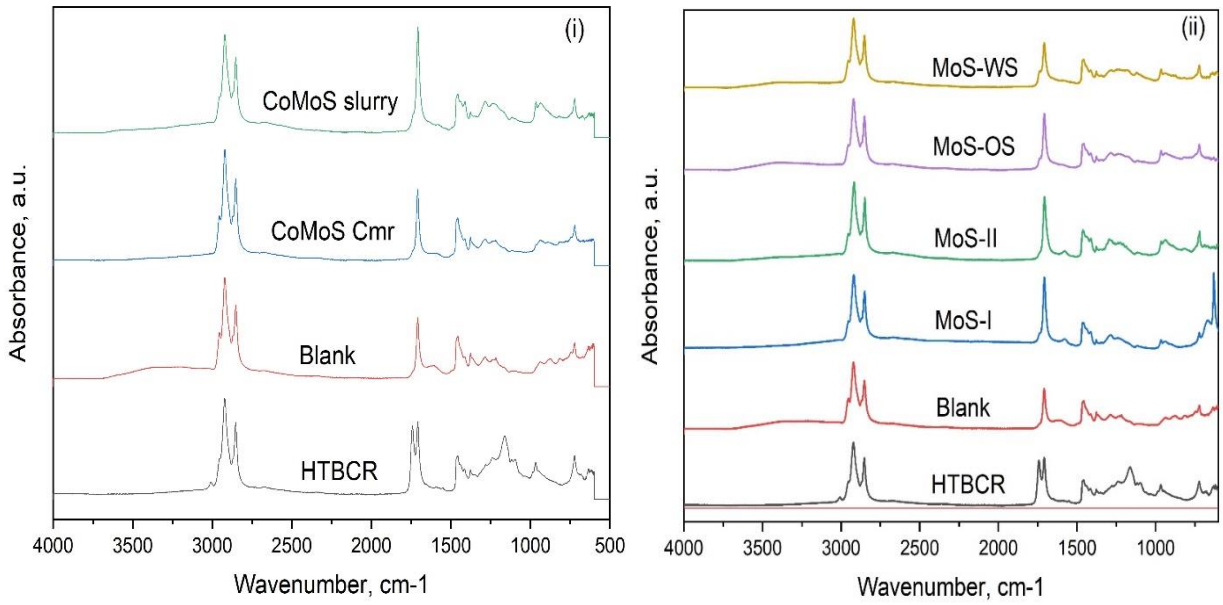

Figure 3.9: *FT-IR spectra of HTBCr and hydrotreated products (i) upgraded products from CoMoS Cmr and CoMoS Slurry catalysts and (ii) upgraded products from metal sulfide-based slurry catalysts.*

3.4.3.2 Oil-Soluble Slurry Phase Dispersed Catalyst

As described above, after the initial catalyst screening using different slurry phase dispersed catalysts, the oil-soluble molybdenum (MoS-OS) catalyst displayed better activities in terms of the reduction of oxygen content and higher yields of liquid product. Therefore, the amount of metal concentration in the catalyst was reduced to the ppm level from the wt% level because slurry phase dispersed catalysts work well in metal ppm concentrations [19-22]. As a result, a series of the test runs were planned on metal (Mo) concentration in the range of 500 to 1700 wppm (0.07–0.23 wt% of catalyst) at a constant reaction temperature (350 °C), pressure (653 psi initial), and time (2 h). The amounts of solid and liquid products recovered are presented in Fig. 3.10 along with the results from the blank run (without a catalyst) for comparison. All catalysts showed better results compared with the blank run. The amount of solids produced with catalysts having 500–1700 wppm of metal (Mo) is in the range of 2.5 to 10 wt%. The catalyst with 1100 wppm of Mo generated the smallest amount of solids (2.5 wt%).

3.4.3.2.1 TGA Analysis

The liquid product recovered from the experimental run using a concentration of 1100 wppm of Mo in the MoS-OS catalyst was analyzed with TGA and is shown in Fig. 3.11. The results showed that upgraded bio-oil contains about 25, 24.5, and 38 wt% of the materials in the temperature range <250, 250–350, and >350 °C, respectively. The product obtained from the blank run contains 11.07 wt% in the temperature range of <250 °C. TGA results confirm that the upgraded bio-oils produced with MoS-OS (1100 wpm Mo) are lighter compared to the blank run and HTBCr.

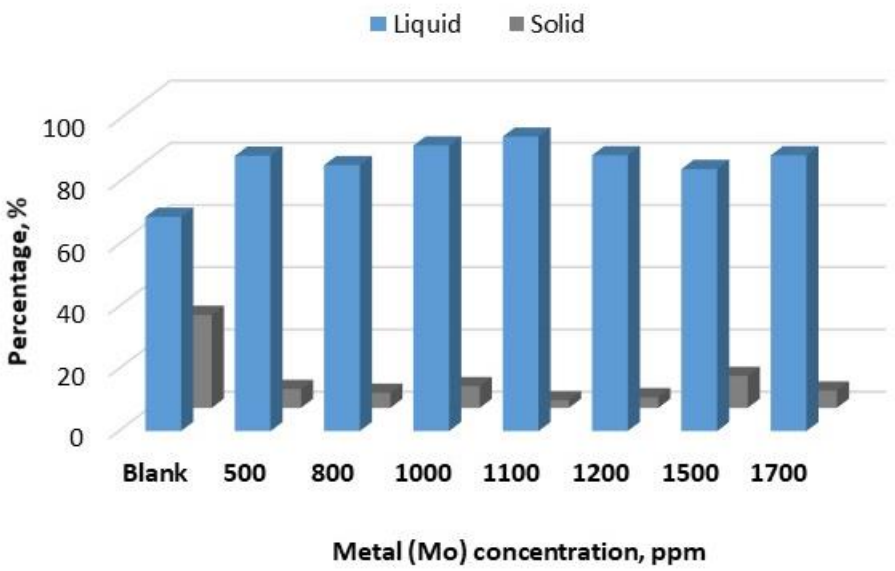

Figure 3.10: *The amount of solid and liquid products obtained after the HTBCr upgrading using MoS-OS (oil-soluble molybdenum slurry catalysts) using different metal concentrations in ppm level. [blank= without catalyst; Reaction conditions: T=350 °C, P=653 psi (initial), and t=2 h]*

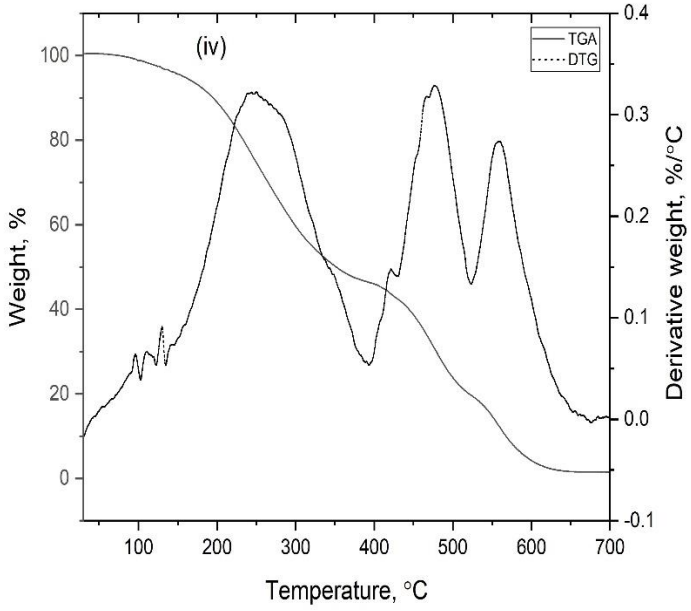

Figure 3.11: *TGA-DTG curves of products from HTBCr upgradation with 1100 wppm of Mo-concentration in MoS-OS catalyst.*

3.4.3.2.2 CHNO Analysis

Properties of the liquid products from the MoS-OS catalyst (with different metal concentrations) are shown in Table 3.10. The catalyst having 1100 and 1500 wppm Mo displayed 58% and 69% HDO conversions, respectively. The calculated HHVs of bio-oils obtained using these catalysts are also higher compared to other catalysts. Although the catalyst having 1500 wppm of metal showed the highest HDO conversion, the amount of solid produced with this catalyst was higher compared to 1100 wppm of the metal MoS-OS catalyst (Fig. 3.10).

3.4.3.2.3 FT-IR Analysis

Fig. 3.12(i) presents the FT-IR analysis of the HTBCr and the liquid products. Similar to the elemental analysis, the high carbon and hydrogen content of HTBCr and liquid products produced a prominent C-H stretch (3000-2840 cm^{-1}), CH_2 bending (1465 cm^{-1}), and CH_3 bending (1375 cm^{-1}). Significant heteroatom functionalities (1700–1100 cm^{-1}) were also observed for all the liquid product samples. For more clarity, Fig. 3.12(ii) shows the FT-IR analysis of HTBCr, blank, and 1100 wppm MoS-OS catalyst experimental runs. In particular, the peak in the region 1650–1700cm^{-1} (carbonyl region) and 1000–1250 cm^{-1} decreased significantly compared to HTBCr and blank runs.

3.4.3.2.4 GC-MS Analysis

Liquid products from the blank run and the catalyst having 1100 wppm of Mo metal in the MoS-OS catalyst were analyzed with GC-MS. The results are shown in Fig. 3.13. The amount of hydrocarbons produced with 1100 wppm of MoS-OS catalyst was higher and the oxygenated compounds produced were lower compared with the blank run (Fig. 3.13(i)). The oxygenates mainly contain hexadecanoic and octadecanoic acids. The aromatics mainly contain benzene and its derivatives. Overall, the amount of hydrocarbons produced with 1100 wppm of MoS-OS catalyst was higher compared with that of the blank run. The product distribution for the hydrocarbons (C6-C28) is shown in Fig. 3.13(ii). The catalyst having 1100 wppm of Mo metal contains mainly C16-C18 hydrocarbons compared to the blank run.

Table 3.10: *Properties of HTBCr and liquid products obtained after HTBCr upgrading using different metal concentrations (500–1700 wppm) in oil-soluble slurry catalyst.*

Properties	**HTBCr**	**Blank**	**Mo-metal concentration in Catalysts, wppm**						
			500	**800**	**1000**	**1100**	**1200**	**1500**	**1700**
Ash content, wt%						1.685			
C, wt%	76.7	77.1	77.9	78.7	78.2	82.9	78.8	83.7	78.2
H, wt%	11.3	11.1	11.9	12.3	12.1	12	12.3	12.6	12.1
N, wt%	0.3	0.2	0.4	0.4	0.3	0.3	0.5	0.2	0.5
O, wt%	11.7	11.7	9.7	8.6	9.3	4.9	8.4	3.6	9.2
H/C, atomic ratio	1.77	1.7	1.8	1.9	1.9	1.7	1.9	1.8	1.9
HDO, wt%	-	0.34	16.8	26.1	20.5	58.3	28.0	69.2	21.3
HHV, MJ/kg	40	39.8	41.6	42.6	42.1	44.3	42.6	45.6	42.0

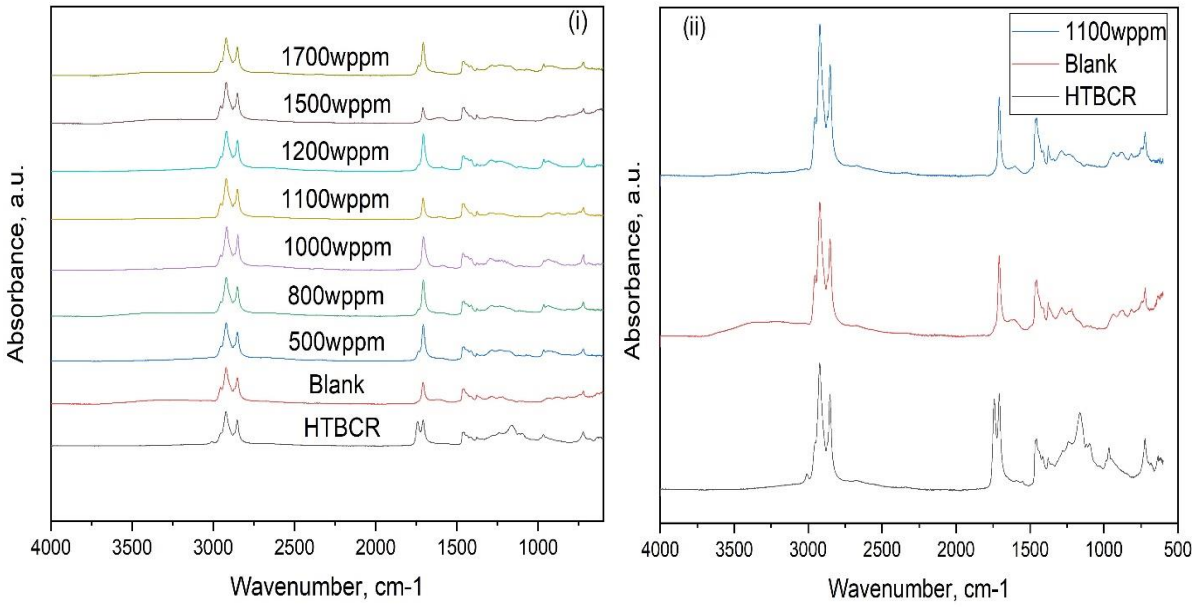

Figure 3.12: *FT-IR analysis of HTBCr and the liquid products recovered (i) after upgradation using different metal concentrations and (ii) after upgradation with 1100 wppm of metal in oil-soluble slurry catalyst (MoS-OS). [blank: without catalyst]*

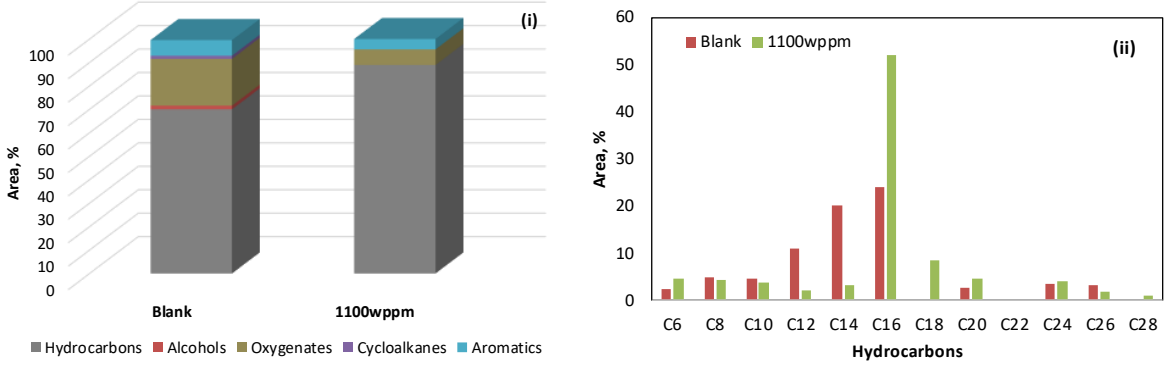

Figure 3.13: *GC-MS analysis of liquid product obtained without catalyst (blank) and with catalyst (1100 wppm of Mo-metal in MoS-OS catalyst) during hydrotreating of HTBCr (i) Area % for hydrocarbons, alcohols, oxygenates, cycloalkanes, and aromatics and (ii) Carbon distribution (C6-C28) in hydrocarbons.*

3.4.3.3 Metal Carbide-based Dispersed Catalysts

The catalyst activities of the metal-carbide-based catalyst, such as NiC and MoC, were also tested for the upgradation of HTBCr crude oil, and the amount of solid and liquid produced is shown in Fig. 3.14. The results revealed that MoC has better catalyst activities for HTBCr upgradation. In the presence of the MoC catalyst, 3 wt% of solid and 96 wt% of liquids were produced. In comparison, the amount of solid produced with the NiC catalyst was 5.4 wt%.

3.4.3.3.1 CHNO Analysis

Properties of the liquid products obtained after HTBCr upgradation using NiC and MoC catalysts are given in Table 3.11. The HDO conversion with NiC and MoC were 10% and 19%, respectively. Although the conversions were higher than for the blank test run, the results were not as good as with the sulfide-based catalysts. The hydrogen/carbon ratio of the products was also improved compared to the blank run.

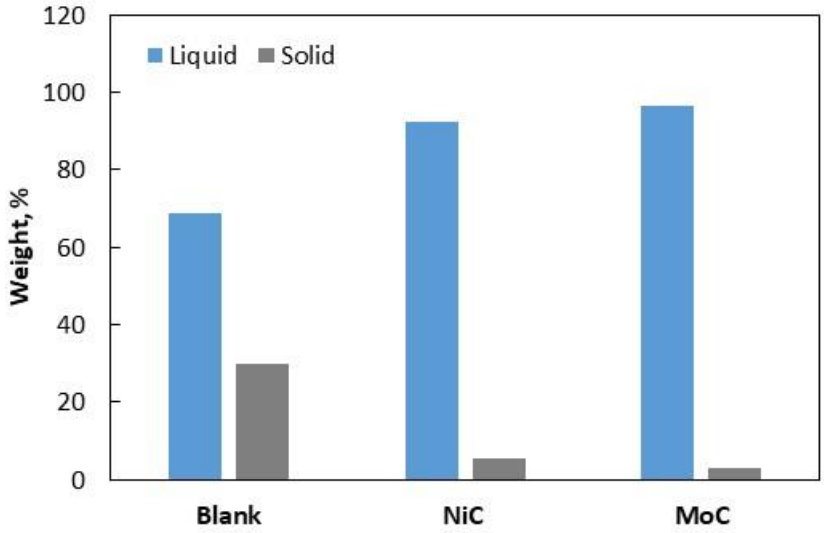

Figure 3.14: *The amount of solid and liquid products obtained after the HTBCr upgrading using NiC and MoC catalysts. [Reaction conditions: T=350 °C, P=653 psi (initial), t=2 h, metal, wppm=20,000, catalyst amount=2.71 wt%]*

Table 3.11: *Properties of HTBCr and liquid products obtained after HTBCr upgrading with metal carbide-based slurry catalysts.*

Properties	HTBCr	Blank	NiC	MoC
C, wt%	76.7	77.1	77.4	78.2
H, wt%	11.3	11.1	11.9	12.1
N, wt%	0.3	0.2	0.3	0.2
O, wt%	11.7	11.7	10.5	9.5
H/C, atomic ratio	1.8	1.7	1.8	1.9
HDO, %	-	0.3	10.4	19.14
HHV, MJ/kg	40	39.8	41.2	42.1

3.4.3.3.2 FT-IR Analysis

The FT-IR analysis of HTBCr and liquid products obtained after upgradation with blank and NiC and MoC catalysts is shown in Fig. 3.15. The liquid products showed a prominent C-H stretch (3000–2840 cm^{-1}), CH_2 bending (1465 cm^{-1}), and CH_3 bending (1375 cm^{-1}). Significant heteroatom functionalities (1700–1100 cm^{-1}) were observed for the HTBCr and liquid product from the blank run. However, in the liquid products from NiC and MoC, the intensity of the peaks in the heteroatom region (1700–1000 cm^{-1}) decreased. In particular, the peak in the region 1650–1700 cm^{-1} (carbonyl region) and 1000–1250 cm^{-1} decreased significantly compared to HTBCr and blank runs. This confirms the removal of heteroatoms during the upgradation experiments performed.

3.4.3.3.3 GC-MS Analysis

GC-MS analysis of the liquid products from NiC and MoC are shown in Fig. 3.16. The liquid products from these catalysts mainly contained oxygenates and oleic acid, which was the main oxygenate produced. The results showed that the octadecanoic acid from the feed mostly converted into oleic acid (Fig. 3.16(iii)). The carbon distribution in the hydrocarbon (Fig. 3.16(ii)) largely contained C_{14}-C_{16}, and the product from the NiC catalyst contained more C_{16} hydrocarbons compared to those obtained with MoC.

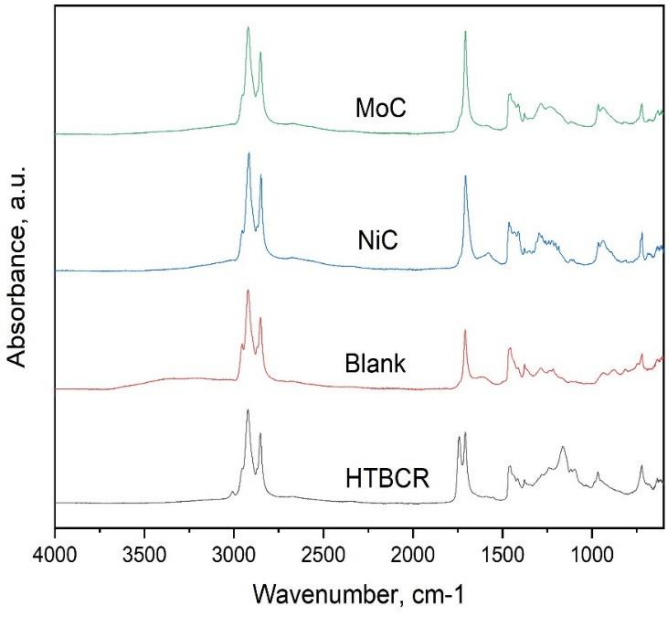

Figure 3.15: *FT-IR spectra of the HTBCr and upgraded products obtained from blank, NiC, and MoC catalysts.*

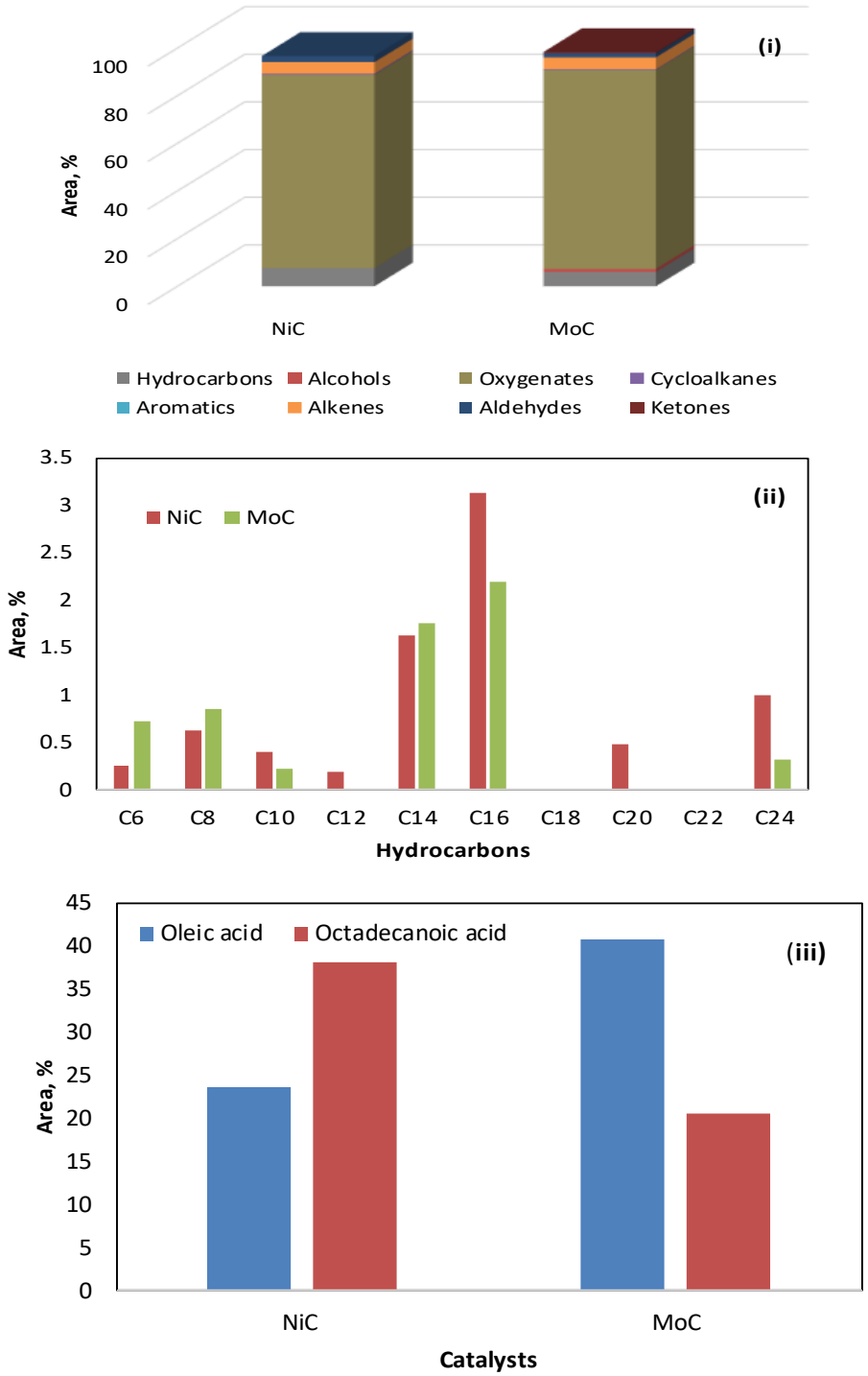

Figure 3.16: *GC-MS analysis of liquid products from NiC and MoC catalysts (i) Area % for hydrocarbons, alcohols, oxygenates, cycloalkanes, and aromatics, (ii) Carbon distribution (C_6-C_{24}) in hydrocarbons, and (iii) Area % for oleic acid and octadecanoic acid.*

3.5 Recommendations

3.5.1 Pyrolysis Biocrude Oil (PBCr-II) Upgrading

The results showed that the upgradation of the pyrolysis biocrude oils is difficult because of the presence of a large amount of phenolic compounds, aldehydes, ketones, acids, and amines. Additionally, the amount of solid produced was in the range of 35 to 38% with the carbide-based slurry catalyst. Reaction optimization studies, including variations in reaction temperature, reaction time, and catalyst amount, are needed to obtain a maximum conversion with pyrolysis biocrude oil.

3.5.2 Hydrothermal Liquefaction Biocrude Oil (HTBCr) Upgradation

In the case of HTBCr upgradation, the oxygen content with the oil-soluble MoS_2 catalysts was reduced significantly. It is worth mentioning that these results were obtained at a 350 °C reaction temperature, 653 psi of initial hydrogen pressure, and 2 h of reaction time, which are lower compared to the literature reports. The reason is that these slurry catalysts are highly dispersed in the feeds, which leads to a better contact between the feed and the catalysts.

In the literature, most of the hydrotreating reactions were performed at higher temperatures of 400–420 °C with a high hydrogen pressure (870–1160 psi). Therefore, the reaction optimization (variation in reaction temperature, pressure, and time) with slurry catalysts can further improve the process with better HDO and upgraded products.

References

1. Huber, G.W., and Corma, A. 2007. Synergies between bio- and oil refineries for the production of fuels from biomass. Angrew Chemie Int. Ed 46: 7184–7201.
2. Bridgwater, A.V. 2012. Review of fast pyrolysis of biomass and product upgrading. Biomass Bioenergy 38: 68–94.
3. Furimsky, E. 2000. Catalytic hydrodeoxygenation: Review. Appl. Catal. A 199: 147–190.
4. Czernik, S., and Bridgwater, A.V. 2004. Overview of applications of biomass fast pyrolysis oil. Energy Fuels 18: 590–598.
5. Choudhary, T.V., and Phillips, C.B. 2011. Renewable fuels via catalytic hydrodeoxygenation. Appl. Catal. A 397 (1−2): 1−12.
6. Adjaye, J.D., and Bakhshi, N.N. 1995. Production of hydrocarbons by catalytic upgrading of a fast pyrolysis bio-oil. Part I: Conversion over various catalyst. Fuel Process. Technol. 45 (3): 161−183.
7. Samolada, M.C., Baldauf, W., and Vasalos, I.A. 1998. Catalyst evaluation for catalytic biomass pyrolysis. Fuel 77 (14): 1667−1675.
8. Vitolo, S., Seggiani, M., Frediani, P., Ambrosini, G., and Politi, L. 1999. Catalytic upgrading of pyrolytic oils to fuel over different zeolites. Fuel 78 (10): 1147−1159.
9. Peng, J., Chen, P., Lou, H., and Zheng, X. 2009. Catalytic upgrading of bio-oil by HZSM-5 in sub- and super-critical ethanol. Bioresour. Technol. 100 (13): 3415−3418.
10. Vispute, T.P., and Huber, G.W. 2009. Production of hydrogen, alkanes and polyols by aqueous phase processing of wood-derived pyrolysis oils. Green Chem. 11 (9): 1433−1445.
11. Vispute, T.P., Zhang, H., Sanna, A., Xiao, R., and Huber, G.W. 2010. Renewable chemical commodity feedstocks from integrated catalytic processing of pyrolysis oils. Science 330 (6008): 1222−1227.
12. Bridgwater, A.V. 2012. Review of fast pyrolysis of biomass and product upgrading. Biomass Bioenergy 38: 68−94.
13. Huber, G.W., Iborra, S., and Corma, A. 2006. Synthesis of transportation fuels from biomass: chemistry, catalysts, and engineering. Chem. Rev. 106: 4044 –4098.
14. (a) Baker, E.G., and Elliott, D.C. US Patent, 5,180,868, 1993; (b) Laurent, E., and Delmon, B. 1996. Influence of water in the deactivation of a sulfide $NiMo/Al_2O_3$ catalyst during hydrodeoxygenation. J. Catal. 146: 281–291; (c) Centeno, A., Laurent, E., and Delmon, B. 1995. Influence of the support of CoMo sulfide catalysts and of the addition of potassium and platinum on the catalytic performances for the hydrodeoxygenation of carbonyl, carboxyl, and guaiacol-type molecules. J. Catal. 154: 288–298; (d) Furimsky, E., and Massoth, F.E. 1999. Deactivation of hydroprocessing catalysts. Catal. Today 52: 381–495; (e) Shabtai, J.S., Zmierczak, W.W., and Chornet, E. US Patent, 5,959,167, 1999; (f) Viljava, T.R., Komulanien, R.S., and Krause, A.O.I. 2000. Effect of H_2S on the stability of $CoMo/Al_2O_3$ catalysts during hydrodeoxygenation. Catal. Today 60: 83–92.
15. Biller, P., Sharma, B.K., Kunwar, K., and Ross, A.B. 2015. Hydroprocessing of bio-crude from continuous hydrothermal liquefaction of microalgae. Fuel 159: 197–205.
16. Ancheyta, J., Rana, M.S., Furimsky, E. 2005. Hydroprocessing of heavy oil fractions. Catalysis Today 109: 3–15.

17. Bellussi, G., Rispoli, G., Molinari, D., Landoni, A., Pollesel, P., Panariti, N., Millini, R., and Montanari, E. 2013. The role of MoS_2 nano-slabs in the protection of solid cracking catalysts for the total conversion of heavy oils to good quality distillates. Catal. Sci. Technol. 3: 176.
18. Rana, M.S., Ancheyta, J., Maity, S.K., and Rayo, P. 2005. Characteristics of Maya crude hydrodemetallization and hydrodesulfurization catalysts. Catalysis Today 104: 86–93.
19. Panariti, N., Del Bianco, A., Del Piero, G., Marchionn, M., and Carniti, P. 2000. Petroleum residue upgrading with dispersed catalyst. Part 1. Catalysts activity and selectivity. Applied Catalysis A: General 204: 215–222.
20. Prajapati, R., Kohli, K., and Maity, S.K. 2017. Slurry-phase hydrocracking of residue with ultradispersed MoS2 catalyst prepared by microemulsion methods. Energy & Fuel 31: 3905–3912.
21. Prajapati, R., Kohli, K., Maity, S.K., and Sharma, B.K. 2019. Ultrafine reverse micelle catalyst for slurry-phase residue hydrocracking. Catalysis Today (in press).
22. Prajapati, R., Kohli, K., Maity, S.K., and Garg, M.O. 2016. Preparation method of slurry phase organic-inorganic fused hybrid catalysts use for residue hydroprocessing US0288101A1/2016.
23. Chianelli, R.R., Berhault, G., Raybaud, P., Kasztelan, S., Hafner, J., and Toulhoat, H. 2002. Periodic trends in hydrodesulfurization: In support of the Sabatier principal. Applied Catalysis A: General 227: 83.
24. Chianelli, R.R. 2006. Periodic trends transition metal sulfide catalysis: Intuition and theory. Oil Gas Sci. Technol. 61: 503–513.
25. Chianelli, R.R., Berhault, G., and Torres, B. 2009. Unsupported transition metal sulfide catalysts: 100 years of science and application. Catalysis Today 147: 275–286.
26. Tian, Y., He, Y., and Zhu. 2004. Low temperature synthesis and characterization of molybdenum disulfide nanotubes and nanorods. Mater. Chem. Phys. 87: 87–90.
27. Yang, J., Zhang, X., Zhou, X., Hong, Y., Shao, J., Zhang, Y., Yang, Q., and Dong, X. 2018. Controlled synthesis of nickel carbide nanoparticles and their application in lithium storage. Chem. Engg. J. 352: 940–946.
28. Fujieda, S., Shinoda, K., Suzuki, S., and Jeyadevan, B. 2012. Materials Transaction 53(10): 1716–1720.
29. Wang, D., Pan, Z., Wu, Z., Wang, Z., and Liu, Z. 2014. Hydrothermal synthesis of MoS2 nanoflowers as highly efficient hydrogen evolution reaction catalysts. Journal of Power Sources 264: 229–234.
30. Yoosuk, B., Kim, J.H., Song, C., and Ngamcharussrivichai, C. 2008. Highly active MoS2, CoMoS2, and NiMoS2 unsupported catalysts prepared by hydrothermal synthesis for hydrodesulfurization of 4,6-dimethyldibenzothiophene. Catalysis Today 130: 14–23.
31. Hosseinnezhad, S., Fini, E.H., Sharma, B.K., Basti, M., and Kunwar, B. 2015. Physicochemical characterization of synthetic bio-oils produced from biomass: a sustainable source for construction bio-adhesives. RSC Advance 5: 75519-75527.
32. Ferrel, J., Olarte, M.V., and Padmaperuma, A. Development and standardization of techniques for bio-oil characterization. https://www.energy.gov/sites/prod/files/2015/04/f21/thermochemical_conversion_ferrell_252301-3.pdf

33. Chen, W.T., Zhang, Y., Lee, T.H., Wu, Z., Si, B., Lee, C.F., Lin, A., and Sharma, B.K. 2018. Upgrading hydrothermal liquefaction biocrude oil from wet biowaste into transportation fuel. Nature Sustainability 1: 702–710.
34. Cheng, S., Wei, L., Alsowij, M.R., Corbin, F., Julson, J., Boakye, E., and Raynie, D. 2018. In-situ hydrodeoxygenation upgrading of pine sawdust bio-oil to hydrocarbon biofuel using Pd/C catalyst. Journal of the Energy Institute 91: 163–171.
35. Yang, Y., Gilbert, A., and Xu, C. 2009. Hydrodeoxyegnation of bio-crude in supercritical hexane with sulfide CoMo and CoMoP catalyst supported on MgO: A model compound study using phenol. Applied Catalysis A: General 360: 242–249.
36. Su-Ping, Z., Yong-Jie, Y., Wei, R.Z., and Tingchen, L. 2003. Study of hydrodeoxygenation of bio-oil from the fast pyrolysis of biomass. Energy Sources 25: 57–65.

Appendix A: Poster

Poster Presented at Tcbiomassplus2019; The International Conference on Thermochemical Conversion Science: Biomass & Municipal Solid Waste to RNG, Biofuels, and Chemicals (October 7-9, 2019) at The Hyatt Regency O'Hare, Rosemont, IL

BIOCRUDE OIL HYDROTREATING USING SLURRY PHASE CARBIDE AND SULFIDE CATALYSTS

ILLINOIS
Illinois Sustainable Technology Center
PRAIRIE RESEARCH INSTITUTE

Kirtika Kohli and Brajendra K Sharma
Prairie Research Institute - Illinois Sustainable Technology Center (PRI-ISTC)
University of Illinois at Urbana-Champaign, Illinois 61820, United States
Email: kirtika@illinois.edu, bksharma@illinois.edu

ABSTRACT

The catalytic hydrodeoxygenation (HDO) of food waste-derived biocrude oil was investigated to produce renewable hydrocarbons using slurry phase carbide and sulfide catalysts. Experiments were performed in order to evaluate the effectiveness of the slurry phase catalysts for the hydrotreatment of biocrude oils and the results were also compared with the conventional hydrotreating sulfide catalysts supported on alumina. The dispersed catalysts showed very high hydrocracking and HDO activities for the hydrotreatment of biocrude oils. The results revealed that coke formation was effectively eliminated, and the properties of the products have been significantly improved in terms of oxygen content and heating values. The catalyst activities were compared with the commercially used bimetallic $CoMo/Al_2O_3$ catalyst at the same reaction temperature and reaction pressure conditions. The slurry phase catalyst were found to be effective in very low catalyst amount. The experimental results showed that even 2.5 wt% CoMo slurry catalyst led to the both decrease in oxygen content and coke amount. On the contrary, typically 20 wt% of the commercial $CoMo/Al_2O_3$ catalyst was used to achieve 35 % HDO conversions. Further, Mo- and Ni-based carbide dispersed catalysts were tested for the HDT of biocrude oil and MoC catalyst displayed higher activity, however, the activity was less compared to conventional $CoMo/Al_2O_3$ catalyst.

A series of different Mo-based sulfide catalysts i.e., dispersed solid powder, oil-soluble, and water-soluble were prepared and the activities of the catalysts were evaluated at high-temperature high-pressure reaction conditions for the HDT of HTL biocrude oil. Among these, oil-soluble MoS_2 slurry catalyst showed highest activity. Further, oil soluble slurry catalyst was tested using different metal concentration in wppm range and this catalyst was found to be much effective in range of 1100-1700 wppm. The slurry catalysts are highly dispersed in the feedstock which leads to the higher selectivity and conversions. A significant decrease in the oxygen content and increase in liquid product demonstrate the potential use of slurry catalysts for the hydrotreatment of biocrude oils.

CHALLENGES IN BIOCRUDE HYDROCONVERSION PROCESS

Hydrothermal liquefaction (HTL) of waste biomass feedstocks has a better energy return on investment, lower GHG emissions, and higher economic potential compared to lipid extraction and transesterification technologies. Despite continuing research efforts, there are still some significant bottlenecks concerning the technology. Although, the energy recovery in the primary product biocrude oil is high, the quality of biocrude oil is still an issue. Hydroconversion is the most efficient way to convert HTL biocrude oils to distillates suitable for use as transportation fuels. The main challenges in hydroconversion processes for treating the biocrude oils are:

- Biocrude oils obtained after HTL contains around 10-20 % oxygen content[1-7], have poor stability, low heating values, and exhibits a high viscosity at room temperature which limits their utilization as transportation fuels.
- The presence of excess water in the feedstocks lead to the early deactivation of the conventional supported sulfide hydrotreating ($NiMoS/Al_2O_3$ and $CoMoS/Al_2O_3$) catalysts. At the high-temperature and high-pressure conditions, the active sulfide phase of the catalysts converted into less active phase. As a result, the degree of hydrogenation decreases, and this leads to the increase in coke (char) formation. These char deposited on the supported catalysts and hence deactivation by pore mouth plugging is observed.
- Because of the catalyst deactivation, low hydrocarbon yields are obtained due to formation of coke in excess amount.

Conventional $NiMo/Al_2O_3$ or $CoMo/Al_2O_3$ hydrotreating catalysts
- Excess amount of water and oxygen in biocrude oils leads to generation of less active sites on catalysts
- Difficult to access pore (big reactant molecules)
- Rapid formation of coke and hence deactivation

OBJECTIVES

Goal:

Development of a Slurry phase hydrocracking process for the upgradation of biocrude oils to high value transportation fuels.

Objectives:

- Designing of slurry phase dispersed HDO catalysts that leads to lower rate of coke formation.
  Synthesis of different slurry phase catalysts such as solid acid dispersed catalysts, oil-soluble, and water-soluble.
- Evaluation of the activities of the synthesized catalysts using HTL biocrude oil from food-waste at high-temperature high-pressure conditions.
  Catalyst activity evaluation and characterization of the hydrotreated products using CHN, FT-IR, and GC-MS.

HIGH-TEMPERATURE HIGH-PRESSURE (HTHP) REACTOR SET-UP

Slurry phase Catalytic Hydroconversion: 500 mL Parr batch reactor, mini-reactors

Automated temperature regulations with continuous stirring and in-situ sampling port

Conversion Products analyzed by elemental analysis (CHN), GC-MS, and FT-IR

RESULTS

Biocrude from HTL (HTBCr) of Food-waste

Properties of Feedstocks

	Food processing waste from a STP[1]	HTBCr
Crude Protein, wt%	24.3	-
Crude Fat, wt%	19.9	-
Hemicellulose, wt%	26.6	-
Cellulose, wt%	5.1	-
Lignin, wt%	2.9	-
Ash, wt%	6.17	0.37
C, wt%	54	76.73
H, wt%	7.93	11.31
N, wt%	0.57	0.26
O, wt%	37.5	11.71
H/C, atomic ratio	1.76	1.77
HHV, MJ/kg	22.68	40

GC-MS Analysis of HTBCr

Retention Time (RT), min	Compound Name	Area, %
22.92	n-hexadecanoic acid	7.49
23.24	Hexadecanoic acid, ethyl ester	1.36
24.61	9,12 octadecadienoic acid	24.86
24.71	17-octadecynoic acid	16.7
24.83	9,12-octadecadienoic acid	5.16
24.88	(9)-9 octadecenoic acid ethyl ester	3.87
24.94	9,12-octadecadienoic acid	1.07
25.37	9,12 octadecadienoic acid	1.21
24.68	11-octadecenoic acid	40.26

HTBCr contains 11 /1 wt% of oxygen content, 1.7 / atomic ratio of H/C, and 40 MJ/kg HHV

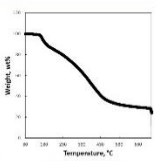

TGA Curve of HTBCr

35 wt% is in <125 °C, 36 wt% in 325-600 °C, and 20 wt% in 600-700 °C boiling range

Molybdenum Sulfide-based Slurry Catalysts

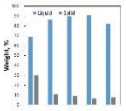

Weight % of Liquid and Solid Products

Properties of Liquid Products

	HTBCr	Blank	MoS-I	MoS-II	MoS-OS	MoS-WS
C, wt%	76.73	77.08	78.71	78.28	79.93	78.22
H, wt%	11.31	11.08	12.02	11.98	12.23	12.29
N, wt%	0.26	0.18	0.21	0.25	0.3	0.68
O, wt%	11.71	11.67	9.07	9.49	7.55	9.01
H/C, atomic ratio	1.77	1.73	1.83	1.84	1.84	1.85
HHV, MJ/kg	40	39.79	42.14	41.87	43.13	42.31

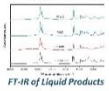

FT-IR of Liquid Products

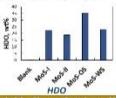

HDO

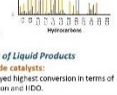

GC-MS Analysis of Liquid Products

Mo-based sulfide catalysts:
Oil soluble Mo-sulfide catalysts displayed highest conversion in terms of less coke formation and HDO.

Bimetallic Catalysts: Comparison between Commercial and Slurry Catalyst

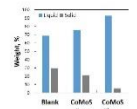

Weight % of Liquid and Solid Products

Properties of Liquid Products

	HTBCr	Blank	CoMoS Cmr	CoMoS Slurry
C, wt%	76.73	77.08	79.71	78.10
H, wt%	11.31	11.08	12.18	11.80
N, wt%	0.26	0.18	0.25	0.22
O, wt%	11.71	11.67	7.77	9.78
H/C, atomic ratio	1.77	1.73	1.85	1.81
HHV, MJ/kg	40	39.79	43.09	41.50

Catalyst amount used:

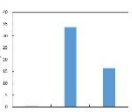

HDO

HDO conversion:
Bimetallic commercial $CoMo/Al_2O_3$ (CoMoS Cmr) and slurry CoMoS (CoMoS Slurry) catalyst showed 34 % and 17 % HDO conversion, respectively. The difference is in the amount of the catalysts used. The low HDO conversion with slurry catalyst was observed because the catalyst used is in percentage amount.

Oil Soluble Slurry Catalysts (MoS-OS)

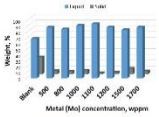

Weight % of Liquid and Solid Products

Properties of Liquid Products

	HTBCr	Blank	500 wppm	800 wppm	1000 wppm	1100 wppm	1200 wppm	1500 wppm	1700 wppm
C, wt%	76.73	77.08	77.86	78.68	78.28	82.85	78.83	83.68	78.23
H, wt%	11.31	11.08	11.87	12.30	12.13	12.00	12.25	12.56	12.06
N, wt%	0.26	0.18	0.43	0.38	0.28	0.27	0.51	0.17	0.51
O, wt%	11.71	11.67	9.74	8.65	9.32	4.89	8.43	3.61	9.21
H/C, atomic ratio	1.77	1.73	1.83	1.88	1.86	1.89	1.87	1.85	1.85
HHV, MJ/kg	40	39.79	41.56	42.61	42.11	44.27	42.61	45.57	42.01

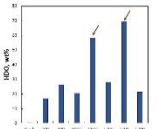

HDO

Metal Carbide-based Slurry Catalysts

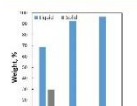

Weight % of Liquid and Solid Products

Properties of Liquid Products

	HTBCr	Blank	NiC	MoC
C, wt%	76.73	77.08	77.41	78.18
H, wt%	11.31	11.08	11.85	12.15
N, wt%	0.26	0.18	0.26	0.23
O, wt%	11.71	11.67	10.49	9.46
H/C, atomic ratio	1.77	1.73	1.84	1.86
HHV, MJ/kg	40	39.79	41.21	42.05

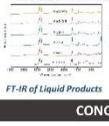

FT-IR of Liquid Products

HDO

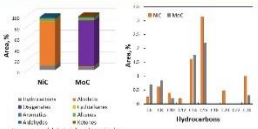

GC-MS Analysis of Liquid Products

Carbide catalysts:
MoC catalyst showed higher conversion than NiC. In the presence of NiC catalyst, most of the oxygenates from HTBCr are converted into alcohols

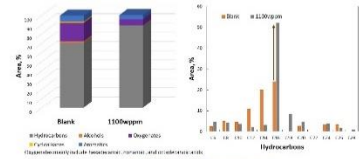

GC-MS Analysis of Liquid Products

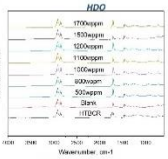

FT-IR of Liquid Products

Mo-based oil-soluble sulfide (MoS-OS) catalysts:
1100 wppm of the Mo metal in MoS-OS catalyst revealed higher HDO conversion with higher production of liquid product. Although, 1500 wppm of the metal displayed highest HDO conversion however, the coke formation is high compared to 1100 wppm of the metal concentration used. The liquid product mainly contains distillate fractions.

CONCLUSIONS & FUTURE WORK

Conclusions:

- Oil-soluble Mo-Sulfide slurry catalysts are the most suitable for the upgradation of the biocrude oils in the presence of 1000-1700 wppm of the metals. Strong improvements in terms of conversion, efficiency, and product quality have been obtained. The HHV values and the H/C ratio of the liquid products improved compared to feedstock and blank run (without catalyst). The liquid products mainly contains the hydrocarbons in the distillate range i.e., C12-C16.
- The application of the slurry hydrocracking technology will allow the production of good-quality transportation fuels. Because of the lesser amount of the catalyst used and low cost of the metals (in wppm concentration) used for the preparation of slurry catalysts, the operating cost of the biocrude oil hydrotreating processes will reduce.

Future Work:

- Reaction optimization studies based on the reaction temperature, reaction pressure, reaction time, different biocrude oils using slurry phase hydrocracking technology.
- Evaluation of catalyst recycling studies.

SLURRY PHASE HYDROCRACKING

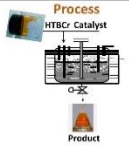

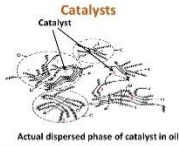

Actual dispersed phase of catalyst in oil

- Slurry processes are much reliable to achieve high conversion and to minimize the yield of low value by-products (coke and gas).
- The metal concentrations used is in catalysts are in wppm level.
- Catalysts dispersed homogeneously with the feedstock and are easily accessible to large oxygenated polyaromatic molecules.
- Catalysts have higher intrinsic stability compared to conventional hydrocracking catalysts. As a results, there is maximum interaction with oil and hydrogen.
- High degree of catalytic metal utilization enables the approach of large complex molecules to reach active sites rather than plug the pores, as in case of supported catalysts, with an effective and strong inhibition of coke formation.

REFERENCES

1. Chen WT, Zhang Y, Lee TH, Wu Z, Si B, Lee CF, Lin A, and Sharma BK, Nature Sustainability 1, 2018, 702-710.
2. Biller P, Sharma BK, Kunwar B, and Ross AB, Fuel 159, 2015, 197-205.

ACKNOWLEDGMENTS

- Financial support was provided by ISTC Hazardous Waste Research Funds.
- The authors acknowledge the School of Chemical Sciences, University of Illinois at Urbana-Champaign for CHN analysis.
- The authors thank Tim Leon for reactor set-up help and Lee Green for running the GC-MS analysis